

VILNIUS UNIVERSITY

Domas Paipulas

**REFRACTIVE INDEX MODIFICATION IN GLASSES  
AND CRYSTALS WITH ULTRASHORT LASER PULSES**

Summary of doctoral dissertation  
Physical sciences, Physics (02P)

Vilnius 2011

The doctoral dissertation was prepared during 2007 – 2011 in Vilnius University. Part of the experiments were done in Shizuoka University (Hamamatsu, Japan)

**Scientific supervisor:**

*Prof. habil. Dr. Valdas Sirutkaitis (Vilnius University, Physical sciences, Physics – 02P)*

**Scientific advisor:**

*habil. Dr. Virgilijus Vaičaitis (Vilnius University, Physical Sciences, Physics – 02P).*

Doctoral committee:

**Chairman:**

1. *Prof. habil. Dr. Algis Petras Piskarskas (Vilnius University, Physical sciences, Physics - 02P)*

**Members:**

2. *Dr. Eugenijus Gaižauskas (Vilnius University, Physical Sciences, Physics - 02P)*
3. *Prof. habil. Dr. Eugenijus Šatkovskis (Vilnius Gediminas Technical University, Physical sciences, Physics- 02P)*
4. *Prof. habil. Dr. Algirdas Audzijonis (Vilnius Pedagogical University, Physical sciences, Physics - 02P)*
5. *Prof. habil. Dr. Audrius Dubietis (Vilnius University, Physical Sciences, Physics - 02P)*

**Opponents:**

1. *Prof. habil. Dr. Rimas Vaišnoras (Vilnius Pedagogical University, Physical Sciences, Physics - 02P)*
2. *Dr. Ramūnas Adomavičius (Center for Physical Sciences and Technology, Semiconductor Physics Institute, Physical sciences, Physics- 02P, Semiconductor Physics - P265)*

The dissertation will be defended under open consideration in the Council of Physics on the 11<sup>th</sup> of November, 2011, 2 p.m. at the Faculty of Physics of Vilnius University, room 510. Address: Saulėtekio ave. 9, LT - 10222, Vilnius, Lithuania.

The summary of the dissertation was distributed on the 11 of October, 2011. The dissertation is available at Vilnius University Library and the library of the Institute of Physics.

VILNIAUS UNIVERSITETAS

Domas Paipulas

**LŪŽIO RODIKLIO MODIFIKAVIMAS STIKLUOSE IR  
KRISTALUOSE VEIKIANT ULTRATRUMPAISIAIS  
LAZERIO IMPULSAIS**

Daktaro disertacijos santrauka  
Fiziniai mokslai, fizika (02P)

Vilnius 2011

Disertacija rengta 2007–2011 metais Vilniaus universitete. Dalis eksperimentų buvo atlikta Shizuokos Universitete (Hamamatsu, Japonija).

**Mokslinis vadovas:**

*Prof. habil. Dr. Valdas Sirutkaitis (Vilniaus universitetas, fiziniai mokslai, fizika – 02P)*

**Konsultantas:**

*habil. Dr. Virgilijus Vaičaitis (Vilniaus universitetas, fiziniai mokslai, fizika – 02P).*

**Disertacija ginama Vilniaus universiteto Fizikos mokslų krypties taryboje:**

Doktorantūros komitetas:

**Pirmininkas:**

1. *Prof. habil. Dr. Algis Petras Piskarskas (Vilniaus universitetas, fiziniai mokslai, fizika – 02P)*

**Nariai:**

2. *Dr. Eugenijus Gaižauskas (Vilniaus universitetas, fiziniai mokslai, fizika – 02P)*
3. *Prof. habil. Dr. Eugenijus Šatkovskis (Vilniaus Gedimino technikos universitetas, fiziniai mokslai, fizika – 02P)*
4. *Prof. habil. Dr. Algirdas Audzijonis (Vilniaus pedagoginis universitetas, fiziniai mokslai, fizika – 02P)*
5. *Prof. habil. Dr. Audrius Dubietis (Vilniaus universitetas, fiziniai mokslai, fizika – 02P)*

**Oponentai:**

1. *Prof. habil. Dr. Rimas Vaišnoras (Vilniaus pedagoginis universitetas, fiziniai mokslai, fizika – 02P)*
2. *Dr. Ramūnas Adomavičius (Fizinių ir technologinių mokslų centras, Puslaidininkių fizikos institutas, fiziniai mokslai, fizika – 02P, puslaidininkių fizika – P265)*

Disertacija bus ginama viešame Fizikos mokslo krypties tarybos posėdyje 2011 m. lapkričio 11 d., 14 val., Vilniaus universiteto Fizikos fakultete 510 auditorijoje.  
Adresas: Saulėtekio 9, LT-10222, Vilnius, Lietuva.

Disertacijos santrauka išsiuntinėta 2011 spalio 11 d. Disertaciją galima peržiūrėti Vilniaus universiteto ir Fizikos instituto bibliotekose.

# Introduction

More than a decade ago it was shown, that by tightly focusing femtosecond laser radiation inside the bulk of transparent material, it is possible to induce highly localized structural changes with modified optical properties [1]. Later it was shown, that depending on laser pulse intensities these changes can manifest as uniform zones of modified refractive index [1], lead to birefringent zone formation [2] or void-like structure creation if intensities are above the material damage threshold [3]. Reasons for such material modification are still not well understood. It is known that the key process of this interaction is nonlinear light absorption that takes place in transparent materials when laser pulse has high intensity and short duration. Several absorption mechanisms were identified: multiphoton, tunnel and avalanche ionization. Strong light absorption that happens only in a confined volume, deep in the bulk of the material, creates extreme conditions responsible for changes of material's structural composition. Ultrafast heating and rapid cooling under the high stress initiates resolidification and densification of pulse-affected zones thus forming regions with modified refractive index [4]. Other physical phenomena, like color center formation [5], participate in the process complicating full understanding of physics happening during material modification. Even if complete picture of this phenomenon is yet to be understood, striking applications that employ transparent material modification emerge day by day. By moving focused laser beam through a material, various photonic elements and devices were demonstrated: waveguides [1], diffractive components [6], data storage elements [3], and even, with the aid of chemical treatment, complicated microchannel networks [7].

However, most of these modification experiments were performed with traditional ultrashort laser systems based on Ti:sapphire material. These laser systems are known for the high quality and short duration pulses, however, the nature of Ti:sapphire material makes laser pumping process quite complicated and not reliable in harsh industrial applications. In recent years a great amount of interest has grown towards Yb:KGW laser systems. These lasers are more straightforward, robust, and are capable to produce intense laser pulses at high repetition rates that are double-beneficial for industrial world. However, such lasers produce pulses that differ from these generated with Ti:Sapphire systems in the sense of pulse duration and wavelength. Thus it is unknown if these pulses can induce similar material modifications in amorphous material. So the **main task** of this thesis was to investigate the possibility to induce material modifications that has smooth, nondestructive refractive index changes in the transparent materials using Yb:KGW laser system. The research was not only limited to amorphous materials. Modification inducing was also carried out in crystalline materials. Capability to form various photonic structures inside the crystals could open new scientific opportunities. Surprisingly, investigations of crystal modification with laser pulses are very scarce.

## Tasks

During thesis preparation period the following tasks were completed:

1. Fused silica modification experiments using ultrashort, high repetition rate laser pulses. Writing pulse parameters influence on the optical properties of modified materials. Determination of optimal pulse parameters required for writing of nondestructive, stable modifications with altered refractive index changes in fused silica glass.
2. Investigation of possibility to write refractive index modifications in nonlinear crystals, such as lithium niobate and KDP with the ultrashort laser inscription method.
3. The use of ultrashort laser pulses for inducing photorefractive modifications in lithium niobate crystals. The investigation of possibility to use this effect for data manipulation purposes in photorefractive materials.
4. The research of the modification influence on the third order nonlinear effects taking place in the fused silica glass.
5. Efficient photonic device, such as volume Bragg grating, inscription in transparent materials using direct laser writing technique.

## Novelty

1. It was demonstrated for the first time, that ultrashort pulses from Yb:KGW laser system can be used for the formation of permanent modifications with altered refractive index in fused silica and lithium niobate crystal. It was showed that accumulation effects fate the homogeneity of created modifications in fused silica.
2. It was identified, that with ultrashort laser pulses it is possible to induce photorefractive modifications in pure and iron-doped lithium niobate crystals. It was demonstrated for the first time, that femtosecond pulses can induce anomaly high refractive index changes in these crystals. Also, completely three-dimensional data recording and erasing technique using femtosecond laser pulses was demonstrated, reasons that prevent multiple data rewriting were identified in these crystals.
3. For the first time the volume Bragg gratings made with direct laser writing technique and having record-high diffraction efficiencies for this writing technique were demonstrated in lithium niobate crystal. These results show that lithium niobate is suitable material for three-dimensional photonic device recording that can be used for linear and nonlinear photonic applications.
4. It was demonstrated experimentally, that modifications induced in fused silica glass influence third order nonlinear effects happening during the interaction of intense pulse with the material. It was showed, that supercontinuum spectrum

shrinks and its intensity drops when material modifications start to appear. Also filament splitting along the beam path was observed in the material. This effect resulted in inhomogeneous distribution of modified material.

## Practical value

Results presented in this thesis are beneficial not only for fundamental understanding of light and mater interaction, but are also important for industrial applications. It was shown, that with Yb:KGW laser system *Pharos* it is possible to create integrated photonic elements in the bulk of glass or even some crystalline materials, without effecting the surface of processed material. Also it was demonstrated that such photonic elements (in our case volume Bragg gratings) could have high efficiencies, making this inscription technique attractive for new device creation. It was shown, that such high pulse repetition rate system could decrease the time required for device fabrication by a magnitude if compared to convenient Ti:sapphire systems. Also, the prospect of lithium niobate crystal as a data storage material where each information bit can be selectively recorded and erased using ultrashort laser pulses was revealed.

## Statements to defend

1. Using high repetition rate ultrashort pulses, generated with Yb:KGW laser system, it is possible to induce refractive index changes in fused silica. Such modifications have birefringent effect and their homogeneity is fated by accumulation effects that are present in the material.
2. With ultrashort laser pulses it is possible to induce permanent refractive index changes in lithium niobate crystal. The change in refractive index is caused by the crystal amorphization. In other hand, no smooth modifications can be created in KDP crystal due to the crystal decomposition.
3. In pure and iron-doped lithium niobate crystal it is possible to induce photo-refractive modifications with ultrashort laser pulses. These modifications have high refractive index changes and can be used for three-dimensional data recording.
4. Laser-induced modifications weaken the third order nonlinear processes in fused silica glass. The supercontinuum spectrum shrinks and its intensity decays, also filament splits along the beam propagation direction due to structural changes induced in the glass material.
5. The change of refractive index induced by the laser pulses, can be evaluated by measuring volume Bragg grating diffraction efficiency dependence on the overall thickness of these gratings.

## Approbation

### Scientific papers related to the topics of the thesis

1. **D. Paipulas**, V. Kudriašov, M. Malinauskas, V. Smilgevičius, V. Sirutkaitis, The Structural modifications induced in lithium niobate and KDP crystals with high repetition rate femtosecond laser pulses, Appl. Phys. A., **104**(3), 769–773(2011).
2. **D. Paipulas**, V. Kudriašov, K. Kuršelis, M. Malinauskas, V. Sirutkaitis, Manufacturing of diffractive elements in fused silica by high repetition rate femtosecond Yb:KGW laser pulses, Lith. J. Phys. **50**, 129–134(2010).
3. **D. Paipulas**, V. Kudriašov, K. Kuršelis, M. Malinauskas, S. Ost, V. Sirutkaitis, Volume Bragg grating formation in fused silica with high repetition rate femtosecond Yb:KGW laser pulses, J. Laser Micro Nanoeng., **5**(3), 218–222 (2010).
4. (non ISI) **D. Paipulas**, V. Kudriašov, K. Kuršelis, M. Malinauskas, S. Ost, V. Sirutkaitis, Volume Bragg grating formation in fused silica with high repetition rate femtosecond Yb:KGW laser pulses, Proc. of LPM(2010).

### Conference presentations, directly related to the topic of the thesis:

- 39th Lithuanian National Conference of Physics, Vilnius, Lithuania. **D. Paipulas**, V. Mizeikis, V. Sirutkaitis, Photorefractive modifications induced in lithium niobate crystal using ultrashort light pulses (2011).
- LPM2011, Takamatsu, Japan. V. Mizeikis, V. Purlys, **D. Paipulas**, S. Juodkaziš, Reversible writing of photorefractive structures in lithium niobate by laser lithography (2011).
- CLEO2011, Munich, Germany. **D. Paipulas**, M. Malinauskas, V. Smilgevičius, V. Sirutkaitis, Permanent volume Bragg grating fabrication in pure lithium niobate crystal using direct laser writing technique (2011).
- ICPEPA7, Copenhagen, Denmark. **D. Paipulas**, V. Kudriašov, M. Malinauskas, V. Smilgevičius, V. Sirutkaitis, The structural modifications induced in lithium niobate and KDP crystals with high repetition rate femtosecond laser pulses (2010).
- LPM2010, Stuttgart, Germany. **D. Paipulas**, V. Kudriašov, K. Kuršelis, M. Malinauskas, V. Sirutkaitis, Volume Bragg grating formation in fused silica with high repetition rate femtosecond Yb:KGW laser pulses (2010).



- Developments in Optics and Communications, Riga, Latvia. **D. Paipulas**, V. Kudriašov, K. Kuršelis, M. Malinauskas, V. Sirutkaitis, Refractive index modifications induced in fused silica with high repetition rate femtosecond laser pulses (2010).
- Mokslas ir visuomenė moderniojoje Europoje, Vilnius, Lithuania. **D. Paipulas**, V. Kudriašov, M. Malinauskas, V. Smilgevičius, V. Sirutkaitis, The structural modifications induced in lithium niobate and KDP crystals with high repetition rate femtosecond laser pulses (2010).
- 38th Lithuanian National Conference of Physics, Vilnius, Lithuania. **D. Paipulas**, V. Kudriašov, K. Kuršelis, M. Malinauskas, V. Sirutkaitis; Modification of fused silica by high repetition rate femtosecond Yb:KGW laser pulses (2009).
- Northern Optics 2009, Vilnius, Lithuania. **D. Paipulas**, V. Kudriašov, K. Kuršelis, M. Malinauskas, V. Sirutkaitis, Manufacturing of diffractive elements in fused silica by high repetition rate femtosecond Yb:KGW laser pulses (2009).
- Lasers and Optical Nonlinearity 2009, Vilnius, Lietuva. **D. Paipulas**, V. Kudriašov, K. Kuršelis, M. Malinauskas, V. Sirutkaitis, Manufacturing of diffractive elements in fused silica by high repetition rate femtosecond Yb:KGW laser pulses (2009).

#### Other scientific papers:

- **D. Paipulas**, R. Grigonis, V. Staliulionis, V. Sirutkaitis, Group-delay dispersion measurements of laser mirrors using white-light interferometry, Proc. of SPIE, **6596**, 659614–1 (2007).
- M. Malinauskas, H. Gilbergs, A. Žukauskas, V. Purlys, **D. Paipulas** and R. Gadonas, A femtosecond laser-induced two-photon photopolymerization technique for structuring microlenses, J. Opt. **12**(3), 035204(1–8) (2010).
- A. Žukauskas, M. Malinauskas, L. Kontenis, V. Purlys, **D. Paipulas**, M. Vengris and R. Gadonas, Doped polymeric microstructures for optically active functional devices, Lith. J. Phys. **50**(1), 55–61 (2010).
- M. Malinauskas, G. Bičkauskaitė, M. Rutkauskas, V. Purlys, **D. Paipulas** and R. Gadonas, Self-polymerization of nano-fibers and nano-membranes induced by two-photon absorption, Lith. J. Phys. **50**(1), 135–140 (2010).
- M. Malinauskas, P. Danilevičius, D. Baltriukienė, M. Rutkauskas, A. Žukauskas, Ž. Kairytė, G. Bičkauskaitė, V. Purlys, **D. Paipulas**, V. Bukelskienė and R. Gadonas, 3D artificial polymeric scaffolds for stem cell growth fabricated by femtosecond laser, Lith. J. Phys. **50**(1), 75–82 (2010).

- M. Malinauskas, H. Gilbergs, A. Žukauskas, K. Belazaras, V. Purlys, P. Danilevičius, M. Rutkauskas, G. Bičkauskaitė, **D. Paipulas**, R. Gadonas, A. Gaidukevičiūtė, I. Sakellari, M. Farsari and S. Juodkasis, Femtosecond laser polymerization of hybrid/integrated micro-optical elements and their characterization, *J. Opt.* **12**, 124010(1–9) (2010).
- K. Kuršelis, T. Kudrius, **D. Paipulas**, O. Balachninaite, V. Sirutkaitis, Experimental study of femtosecond laser micromachining of grooves in stainless steel, *Lith. J. Phys.* **50**(1), 95–103 (2010).
- M. Malinauskas, H. Gilbergs, A. Žukauskas, K. Belazaras, V. Purlys, M. Rutkauskas, G. Bičkauskaitė, A. Momot, **D. Paipulas**, R. Gadonas, S. Juodkasis and A. Piskarskas, Femtosecond laser fabrication of hybrid micro-optical elements and their integration on the fiber tip, *Proc. SPIE*, **7716–9** (2010).
- M. Malinauskas, V. Purlys, A. Žukauskas, G. Bičkauskaitė, T. Gertus, P. Danilevičius, **D. Paipulas**, M. Rutkauskas, H. Gilbergs, D. Baltriukienė, L. Bukelskis, R. Širmenis, V. Bukelskienė, R. Gadonas, V. Sirvydis and A. Piskarskas, Laser two-photon polymerization micro- and nanostructuring over a large area on various substrates, *Proc. SPIE*, **7715–49** (2010).
- M. Malinauskas, A. Žukauskas, G. Bičkauskaitė, M. Rutkauskas, K. Belazaras, H. Gilbergs, P. Danilevičius, V. Purlys, **D. Paipulas**, T. Gertus, R. Gadonas, A. Piskarskas, D. Baltriukienė, V. Bukelskienė and A. Gaidukevičiūtė, Fabrication of Three-Dimensional Nanostructures by Laser Polymerization Technique, *Proc. CYSENI* (2010).
- P. Danilevičius, A. Žukauskas, G. Bičkauskaitė, V. Purlys, M. Rutkauskas, T. Gertus, **D. Paipulas**, J. Matukaitė, D. Baltriukienė and M. Malinauskas, Laser 3D micro/nanofabrication of polymers for tissue engineering applications, *Latvian J. Phys. Tech. Sci.*, **48**(2), 32–43 (2010).
- M. Malinauskas, V. Purlys, A. Žukauskas, M. Rutkauskas, P. Danilevičius, **D. Paipulas**, G. Bičkauskaitė, L. Bukelskis, D. Baltriukienė, R. Širmenis, A. Gaidukevičiūtė, V. Bukelskienė, R. Gadonas, V. Sirvydis and A. Piskarskas, Large scale laser two-photon polymerization structuring for fabrication of artificial polymeric scaffolds for regenerative medicine, *Proc. AIP*, **1288**, 12–17 (2010).

## Contributions

Most of the experiments described in this thesis were performed in Vilnius University, Laser Research Center during the period from 2008-2011 under the supervising of prof. V. Sirutkaitis. Part of the experiments, considering the photorefractive modifications induced in lithium niobate crystals were performed in Shizuoka University, Japan, during the internship visit in 2011.01-2011.02 under supervising of dr. V. Mizikis. All experiments and modeling described in this dissertation were performed

by the author himself; however, it is important to distinguish the contribution from these co-authors:

- **prof. V. Sirutkaitis** supervised the research progress and helped to build experiments, participated in data analyses and interpretation, helped to present results to scientific community;
- **prof. V. Smilgevičius** consulted on various nonlinear processes such as second harmonics generation happening in lithium niobate crystals;
- **dr. V. Kudriašov** helped to understand the physics behind transparent material modification phenomena; consulted on data interpretation, helped to perform experiments concerned with fused silica modification with ultrashort pulses;
- **dr. V. Mizeikis** introduced to photorefractive phenomenon and helped to perform experiments and analyze data concerning to photorefractive modification inducing in lithium niobate crystals;
- **dr. M. Malinauskas** helped to analyze data and helped during data preparation process;
- students **S.Ost, K.Kuršelis** helped to perform some experiments.

Also valuable suggestions during experimental and data analyses were received from *dr. M.Vengris* and *dr. A.Melninkaitis*, discussions about nonlinear processes taking place in the fused silica were helpful with *dr. E. Gaižauskas, dr. G. Valiulis, dokt. V. Jukna*; for the introduction to diffraction grating physics I am grateful to *dr. V. Vaičaitis*; the importance of nonlinear crystal modifications and its wide applicability was elucidated by *prof. A. P. Piskarskas*.

## Structure of the thesis

This thesis is arranged into the four main chapters and also has an introduction in the beginning and conclusions as well as the reference list supplied at the end. In the first chapter, general physical processes considering the modification inducing in transparent materials with ultrashort laser pulses are presented. The electromagnetic wave and transparent material interaction phenomena are described in details. Various possible modification types are classified with examples. Also theoretical models that explain the origin of material modification are depicted. The second chapter is devoted to experiments with fused silica. The experimental setup used for modification purposes and acquired results are described, also the technique for the measuring of refractive index changes using volume Bragg gratings is explained. The third chapter describes the investigation of modification creation in nonlinear crystals. This chapter covers photorefractive and permanent modifications in lithium niobate crystal as well as tests on KDP crystal modifications. The fourth chapter focuses on the modification influence on nonlinear processes in the fused silica glass.

Experiments and results regarding dynamics of supercontinuum spectrum and light filament are presented.

# 1 Modification of fused silica with Yb:KGW laser pulses

Fused silica is one of the most popular optical materials used in modern optics. It has outstanding optical and physical properties: has high transmittance in the broad spectral range (0.180-2,1  $\mu\text{m}$ ), low thermal expansion, high laser damage threshold. This material become irreplaceable for manufacturing various elements used for laser physics, fibers, photolithography, semiconductor physics and various other spheres.

Fused silica (also called fused quartz) is amorphous state of silica crystal consisting of silicon dioxide tetrahedral linked in the ring-like structures. Depending on the manufacturing conditions several types of fused silica glasses can be manufactured. The highest quality glass is, usually, produced using flame-fusion technique. Such glass has very high transmittance in UV range and almost has no excess of metallic impurities and is widely applicable in optics and laser physics.

A phenomenon of femtosecond pulse modification of fused silica is known for a decade, however, almost no data is present about the modifications induced with the Yb:KGW laser pulses. In the following sections will be presented experimental results on fused silica modifications induced with high pulse repetition rate laser system *Pharos*.

## 1.1 Experimental setup

We used regeneratively amplified Yb:KGW laser (*Pharos*, made by *Light Conversion Ltd.*) as femtosecond laser source. This laser produces high intensity pulses with 1030-nm wavelength, at 300-fs duration and variable frequency up to 300 kHz. The conventional optical setup used in the experiment is shown in Fig. 1.1. Laser pulses are first attenuated and then focused into the bulk of fused silica with a 0.42 numerical aperture (NA) lens, having focal length of 6.24 mm. The sample was mounted on a 3-axis, *Aerotech* based, nanopositioning system (*AltSCA* assembled by *Altechna Ltd.*) having minimal translation step of 10 nm, total positioning accuracy up to 50 nm and repeatability reaching 300 nm. The maximum traveling range was 300 mm/s. In this configuration, the sample position, in respect to the beam focus, could be highly accurate and easily controlled with automatized software (*SCA, Altechna Ltd.*). By selecting the appropriate inscribing algorithm, various kinds of photonic structures could be fabricated in the bulk of the glass material by the means of direct laser writing (DLW) technique.

Used lens was capable to focus 3.9 mm diameter laser beam to 3.1  $\mu\text{m}$  diameter spot at the focus. The confocal length of the focus was 11  $\mu\text{m}$ . In order to minimize

1.1 Table: Main optical and physical properties of fused silica used in experiments.

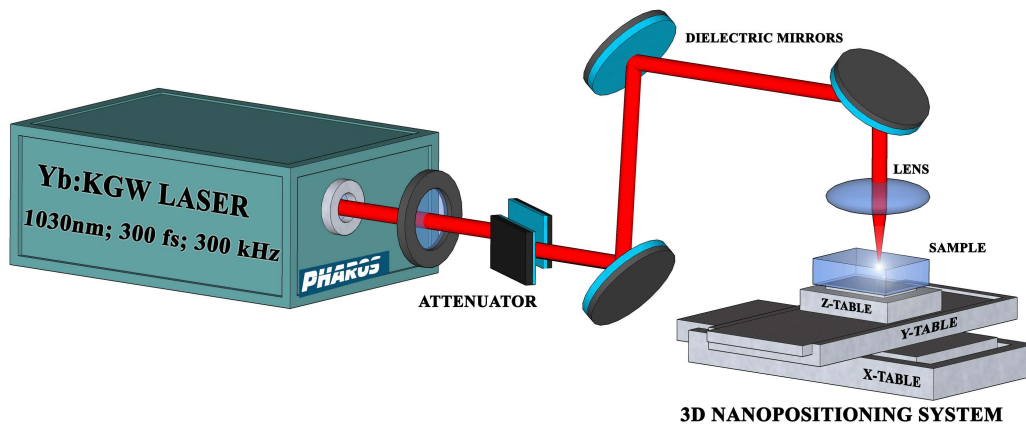
Property	LITHOSIL [8]	KV1 [9]
Density (g/cm <sup>3</sup> )	2.2	2.2
Heat conductivity (W/(mK))	1.31	1.38
Specific heat (J/(gK))	0.79	0.70
Maximum working temperature (°C)	980	1150
Softening point (°C)	1600	1730
Refractive index (1 μm)	1.45	1.45
Transparency range (nm)	160-2300	190-2300
Band gap (eV)	7.5	6.5
Metallic contaminates (10 <sup>-6</sup> )	< 0.1	< 30

the influence of spherical aberrations all structures were written no deeper than 300 μm.

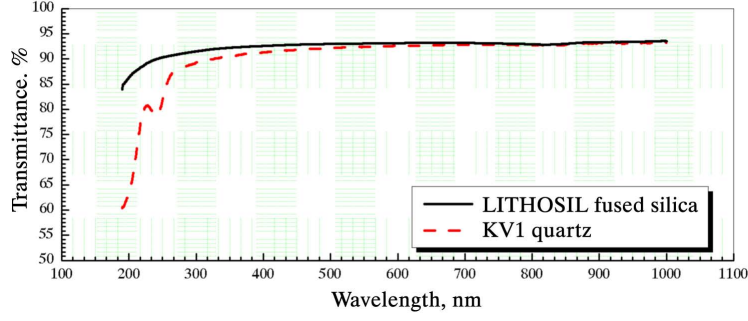
The two types of fused silica were investigated: the ultraviolet silica LITHOSIL, and typical fused quartz made from natural silica KV1. The typical parameters of these materials are shown in 1.1 table and spectral transparency in Fig. 1.2. It is clear from these data that both glasses are almost identical, however the level of metal impurities are much higher in KV1 glass, that reduces the band gap (by 1 eV) and transparency in short wave spectral region.

## 1.2 Modifications in fused silica: parametric analysis

It is assumed, that modification starts to appear in the material when the density of the free electrons (electrons that were excited to the conduction band) reaches specific, so called critical density. Ultrashort, high energy pulses can create such free



1.1 Fig: Optical setup for the glass inscription experiments.



1.2 Fig: The transparency of LITHOSIL and KV1 glasses

electrons in the dielectric materials due to nonlinear absorption processes: multiphoton absorption, tunnel and avalanche ionization. These electrons form spatially confined plasma that could possess distinctive absorption properties. When plasma's density becomes high, this substance could start to absorb the incoming radiation very efficiently and this leads to the material's modification or damage. The critical free electron density could be estimated using Drude-Lorentz theory of the metals, and equals

$$n = \frac{\omega^2 \varepsilon_0 m^*}{e^2}, \quad (1.1)$$

here  $\omega$  is the radiation frequency,  $\varepsilon_0$  - vacuum permittivity,  $m^*$  - reduced mass of the electron and  $e$  is the electric charge. For the 1030 nm wavelength radiation, the critical electron density should be  $1.05 \times 10^{21} \text{cm}^{-3}$ .

The probability to excite the electron through multiphoton absorption could be expressed as [10]

$$w_{df} = \omega k_f^{3/2} \left( \frac{\varepsilon_{osc}}{2\Delta E} \right)^{n_f}, \quad (1.2)$$

here  $k_f = \Delta E / \hbar \omega$ , and  $\varepsilon_{osc}$  is the electron oscillation energy in the field, empirically evaluated as  $\varepsilon_{osc} [\text{eV}] = 9,3 \times 10^{-14} I [\text{W}/\text{cm}^2] \lambda^2 [\mu\text{m}]$  [11], here  $\lambda$  is the laser wavelength.

To evaluate the probability to create the free electron by the means of tunnel ionization is really hard. However in our experiment condition, the Keldysh parameter, expressed as:

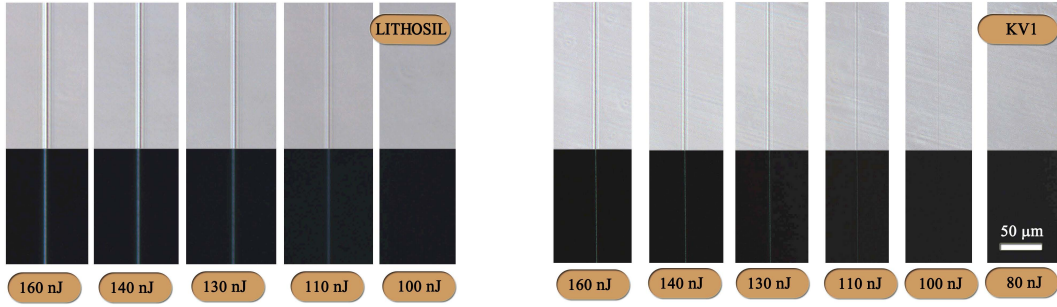
$$\gamma = \frac{\omega}{e} \sqrt{\frac{m c n \Delta E \varepsilon_0}{I}}, \quad (1.3)$$

(here,  $c$  and  $n$  represents the speed of light and refractive index of the material, and  $I$  - the intensity of the laser beam), is close to 1. This means that using ionization theory devised by L. Keldysh [12], the probabilities of multiphoton absorption and tunnel ionization should be comparable.

The avalanche ionization probability could be expressed as [10]

$$w_{lav} \approx 2 \frac{\varepsilon_{osc}}{\Delta E} \frac{\omega^2 \nu_{e-ph}}{\omega^2 + \nu_{e-ph}^2}, \quad (1.4)$$

here  $\nu_{e-ph}$  is electron-phonon momentum exchange rate, that equals  $4,3 \times 10^{13} \text{s}^{-1}$  for



1.3 Fig: Modifications induced in LITHOSIL and KV1 quartz with pulse energies close to modification threshold value. Phase contrast images are shown in the top pictures, while cross-polarized images are presented in the bottom. Pulse repetition rate – 100 kHz, sample translation speed – 0,1 mm/s, modifications are written 100  $\mu\text{m}$  below the surface.

the fused silica [13]. The free electron rate equation could be written as  $dn_e/dt = 2w_{df}n_a + w_{lav}n_e$ , here  $n_a$  – density of atoms, so in this case, when pulse with durations  $\tau$  targets the material, the total electron density will be equal:

$$n_e(I, \lambda, \tau) = \left( n_0 + \frac{2n_a w_{df}}{w_{lav}} \left[ 1 - e^{(-w_{lav}\tau)} \right] \right) e^{(w_{lav}\tau)}, \quad (1.5)$$

here  $n_0$  is initial density of free electrons naturally existing in the material ( $\approx 10^8 \text{ cm}^{-3}$  [14]).

This equation lets to evaluate theoretical light intensity, required for laser-induced modifications. For 300 fs pulse duration and 1030 nm wavelength this intensity equals to  $1.13 \times 10^{13} \text{ W/cm}^2$ . Such intensity in LITHOSIL glass is reached in the focus of 0.42 NA lens if the pulse energy is 120 nJ, or 12 mW power if pulse repetition rate is 100 kHz (in KV1 the energy and power are 80 nJ and 8 mW, respectfully). Self-focusing peak power for fused silica is 3.3 MW, so filamentation regime is reached only when pulse energy is  $> 1 \mu\text{J}$ .

Modification experiments were carried out in fused silica by forming separate lines in the bulk of the material and investing it's morphology with optical microscope. The average beam power was measured before the lens with *Ophir* thermal power sensor (3A). The transmittance of the lens was 83 % and the reflection from the sample surface accounted for 3 % losses. The microscope used in experiment was *Olympus BX51* equipped with phase contrast and cross-polarization measuring regimes.

Typical lines formed with pulse energies close to the modification threshold are shown in Fig. 1.3. Optically detectable modifications in LITHOSIL glass start to appear when pulse energy reaches 110 nJ (energy density  $3.1 \text{ J/cm}^2$ ), while for KV1 quartz – 100 nJ ( $2.8 \text{ J/cm}^2$ ). These values are in good match with theoretical values. The modification threshold dependence on pulse repetition rate (in range 25–300 kHz) was not observed in our experiments.

The morphology of the induced lines starts to change when pulse energy is inc-



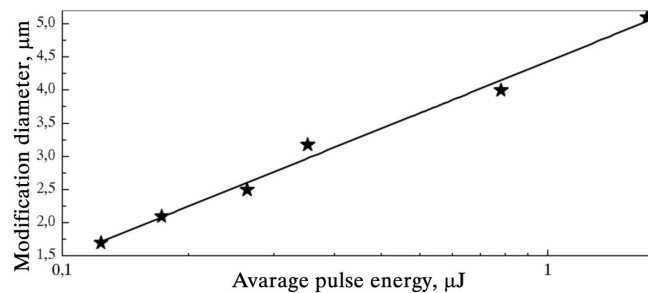
reased. The modification diameter begins logarithmically grow (Fig. 1.4) with the pulse intensity and the homogeneity tends to worsen. When pulse energy is lower than 400 nJ, inscribed line diameter becomes smaller than focused beam diameter. This shows the nonlinear nature of the modification appearance. Microscope images, made in cross-polarization regime shows that even with smallest energies induced modifications possess birefringence (Fig. 1.5), so all these are Type II modifications.

The big drawback of DLW technique used for transparent material processing is the slow fabrication speed. Using conventional 1 kHz laser system, the sample could not be translated faster than 1 mm/s, as otherwise modified regions could not overlap. As single-pulse induced modifications do not possess good characteristics, multipulse treatment are required for the uniform remelting of affected. So in practice, the optimal scanning speed is lower and reaches only tenths or even hundredths of millimeters per second.

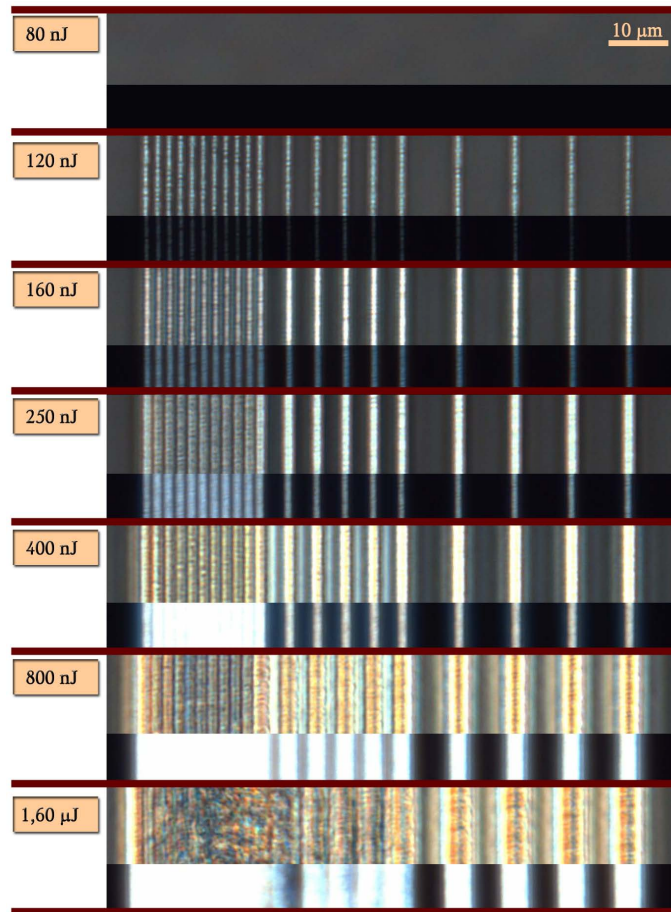
The influence of scanning speed on the modification morphology is demonstrated in Fig. 1.6. It is clear that, besides high repetition rate (in this case 100 kHz), fast sample translation speeds completely destroys line homogeneity. Only when scanning speed is less than 1 mm/s smooth structures can be fabricated. This clearly demonstrates the accumulation effect: knowing that single-pulse modified zone is 1  $\mu\text{m}$  in diameter, the minimum number of pulses required to affect processed zone should be no less than 100 in order to get continuously modified lines. This ratio does not depend on the pulse repetition rate at least up to 300 kHz. At 5 kHz the maximum scanning speed was found to be 50  $\mu\text{m}/\text{s}$ , while at 300 kHz it was 3 mm/s. This suggests that accumulation effect is not linked with cumulative heating at the focal position, as time scale is too long and during pulse-to-pulse arrival time, material is capable to dissipate all acquired heat.

This accumulation effect is closely linked to the formation of nanoperiodic gratings in the bulk of the glass. When the sample translation speed increases, the birefringent effect of the inscribed structures decreases and becomes non-regular. This suggests that when exposition time (number of pulses) is too short, nanogratings formation is no even.

Optical microscopy is not capable to observe nanometric size objects. If the structures are formed on the surface of the glass, it is possible to observe these na-

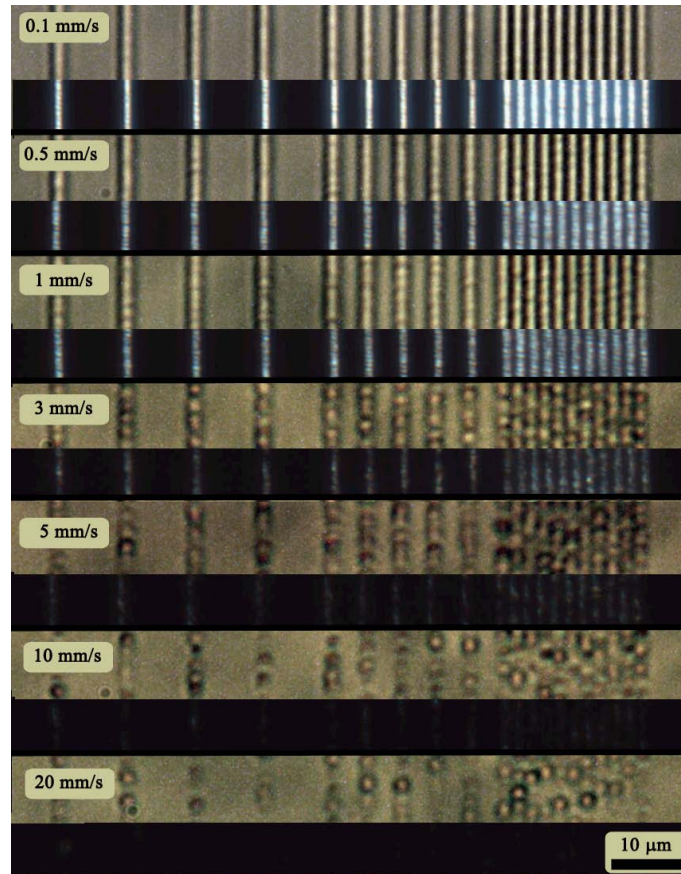


1.4 Fig: Modification diameter dependence on the writing pulse energy. LITHOSIL glass, sample translation speed – 0,1 mm/s, pulse repetition rate – 100 kHz.



1.5 Fig: Modifications induced in fused silica at various pulse energies. Sample translation speed is 0.1 mm/s, focusing lens – 0.42 NA, repetition rate – 100 kHz, polarization – parallel to scanning direction. Line groups in the left are separated by 10  $\mu\text{m}$ , in the middle by 5  $\mu\text{m}$ , in the right 2  $\mu\text{m}$ . Samples were written 200  $\mu\text{m}$  below the surface. Top images made in phase contrast regime, bottom in cross-polarized regime.

nogratings with the help of electron microscope. Such nanogratings are shown in the Fig. 1.7. It is important to stress, that in order to observe these structures, microscope has to work in back scattering electron (BSE) regime. No gratings can be observed in laser affected zone when using more common secondary electron (SE) regime. SE regime is used only for surface morphology studies, while BSE regime could identify material's density fluctuations, so black stripes observed in Fig. 1.7 are not nano-cracks, but areas with varied density. Grating orientation is always perpendicular to the polarization of the writing beam and the periodicity is sustained at the distances far longer than focused beam diameter. Grating period when polarization is parallel to the sample translation direction is 260 nm, and the diameter of single strip is < 60 nm. When polarization is perpendicular, the period is slightly greater – 340 nm. Such periods are comparable to ones reported by Bhardwaj et al. [15], however, this group used Ti:sapphire laser system (800 nm wavelength and 50 fs duration laser pulses) as a light source. These results doubt the observation of previous mentioned group that nanograting period could be linked to the radiation

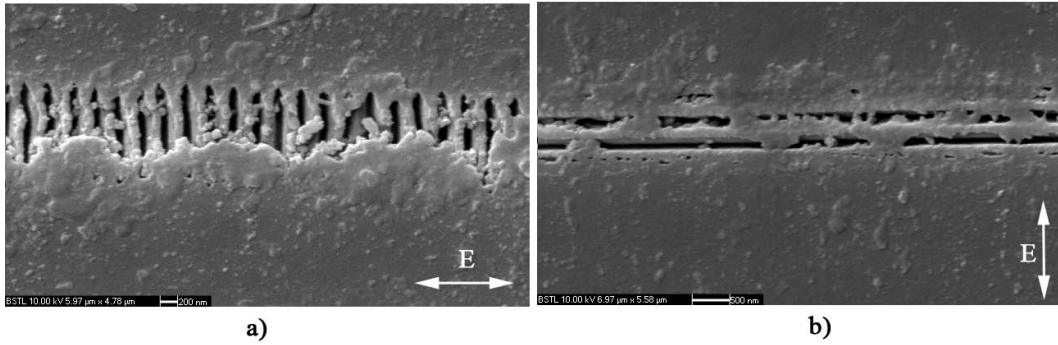


1.6 Fig: Modifications induced in LITHOSIL fused silica at different scanning speeds. Writing pulse energy – 200 nJ, repetition rate – 100 kHz, focused with 0.42 NA lens. Samples were written 200  $\mu\text{m}$  below surface. Top images made in transmittance regime, bottom in cross-polarized regime.

wavelength as  $\lambda/2$ . Also Richter et al. showed that similar period can be achieved with 515 nm wavelength and 450 fs laser pulses [16]. So the grating formation theory based on light and plasma interference effect, suggested by Shimotsuma et al. [17] are doubtful. The explanation of nanograting formation through the plasmonic effects could be more reliable [15], however additional study is still required in order to achieve better understanding about the phenomenon of nanograting formation in the bulk of the fused silica material.

### 1.3 Measuring of the refractive index change: volume Bragg gratings

Measuring of the refractive index changes in micrometer size structures, written in the bulk of the transparent material is not a trivial task. It is possible to use non direct measuring techniques and evaluate refracting index changes from various photonic devices such as waveguides [18] or simple diffraction gratings [19]. However, both these methods are quite imprecise as such photonic elements tend to have low



1.7 Fig: Nanogratings made on the surface of LITHOSIL glass. Sample translation speed  $-10$  mm/s, repetition rate  $-100$  kHz. Pulse polarization in respect to translation direction is: a) parallel and b) perpendicular.

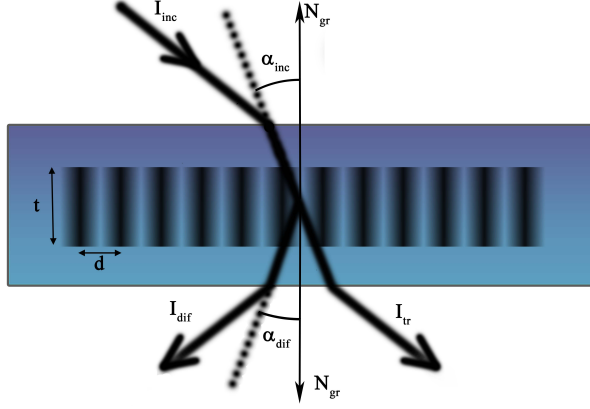
efficiency.

The measuring accuracy can be increased if the photonic element under investigation could have high and from the refractive index dependent efficiency. One type of such elements are volume Bragg gratings (VBG).

Traditionally, commercial VBGs with high diffraction efficiencies are fabricated using holographic technique. The pattern generated by two beam interference process is recorder in photosensitive material. The most popular material used today for such devices is dichromated gelatin (DCG), which has a very high refractive index modulation property ( $\Delta n$  up to 0.1), while retaining good transparency in a broad spectral range. With this technology it is possible to form large area gratings with spatial frequencies up to  $6000$   $\text{mm}^{-1}$ . After the exposure, the gelatin is chemically treated and sandwiched between glass plates for better robustness and handling [20]. A new and very promising material for VBG fabrication is PTR (Photo-Thermo-Refractive) glass. It is a silicate based glass with silver, cerium and fluorine doping. After UV illumination and thermal treatment, it can exhibit a refractive index change of up to  $10^{-3}$ . That change is reasonably smaller than for DCG, but it is more stable and frequencies up to  $10000$   $\text{mm}^{-1}$  can be reached [21].

Several attempts to manufacture VBGs in pure fused silica by means of femto-second laser radiation were reported during the last decade [22, 23]. However the efficiencies of these devices hardly reached 30%. The main problem that researchers encounter is hardly predictable refractive index modification level as the real causes of its appearance are still not clearly identified. This parameter is crucial for the devise efficiency. To our knowledge, the VBGs made in pure fused silica and having highest efficiencies (74.8%) were manufactured by Yamada at al. [23]. These gratings were fabricated by modifying thick regions of the sample using filamentation process. However such technique does not have flexibility to control the modified zone size thus preventing the optimization of fabricating device. Another drawback of this technique is slow fabrication speed – to form a complete, sub-millimeter size grating requires up to six hours or more.

The holographic method for VBG fabrication in pure fused silica glass is quite limited as high laser intensities are required to reach the refractive index modifica-



1.8 Fig: Schematics of transparent volume phase grating. The equally spaced black stripes represent the region of sinusoidally modulated refractive index.

tion regime; however, point by point Direct Laser Writing (DLW) technique can be successfully applied for such device fabrication. This technique has advantages over the holographic method as any desired three-dimensional pattern can be fabricated. However, the manufacturing speed yet could not compete with holographic method.

## 1.4 The diffraction efficiency of VBG

VBGs with high diffraction efficiencies have become an important tool in optical systems, especially in those where spectral and angular selectivity is essential. In contrast with amplitude or profile gratings, diffraction in phase gratings is produced from periodic modulation of the refractive index, created in the bulk of transparent material. The VBGs theory is usually described using a coupled wave model devised by Kogelnik [24].

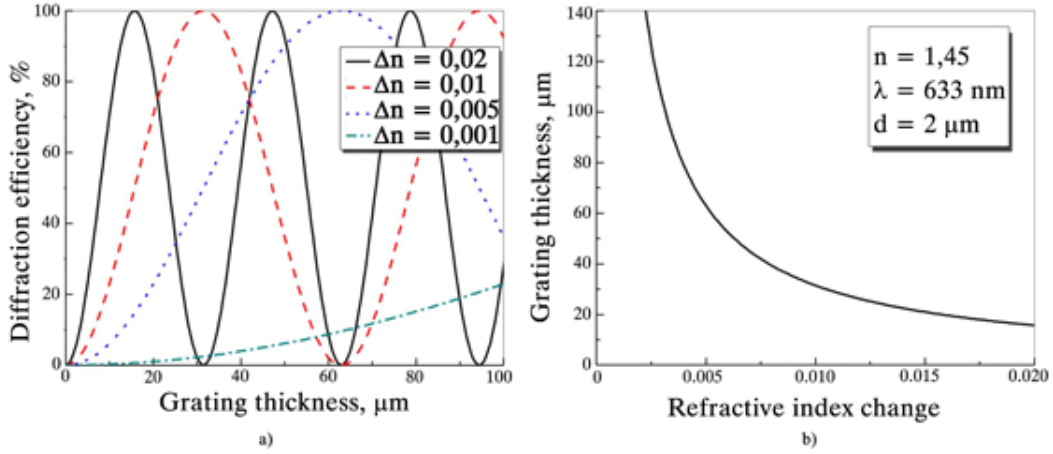
The transmitting grating formed in the bulk of the sample is shown in Fig 1.8. The modulation magnitude is  $\Delta n$ , the period of the grating –  $d$  and the thickness –  $t$ . An incident beam  $I_{inc}$ , enters the grating at angle  $\alpha_{inc}$ . The diffraction condition for this grating is the same as in ordinary surface grating:

$$\frac{m\lambda}{nd} = \sin \alpha_{inc} - \sin \alpha_{dif}, \quad (1.6)$$

here  $m$  is an integer, corresponding to the order of diffraction,  $\lambda$  is wavelength,  $n_{av}$  is the refractive index of the material and  $\alpha_{dif}$  is the angle of diffracted beam. In contrast with ordinary grating, VBG have additional dimension of thickness with which it is possible to control the efficiency of diffracted beam ( $I_{dif}$ ). The VBG diffraction efficiency, described as ratio between diffracted and incident beams, is given by:

$$\eta = \sin^2 \left( \frac{\pi \Delta n t}{\lambda \sqrt{1 - \left(\frac{m\lambda}{2nd}\right)^2}} \right). \quad (1.7)$$

This equation is only valid for angles that are in so called Bragg condition (where



1.9 Fig: a) Diffraction efficiency dependence on grating thickness at various refractive index modulation levels; b) dependence of minimal thickness of volume grating that produces 100 % efficiency on refractive index modulation level.

$$\alpha_{inc} = \alpha_{dif} ).$$

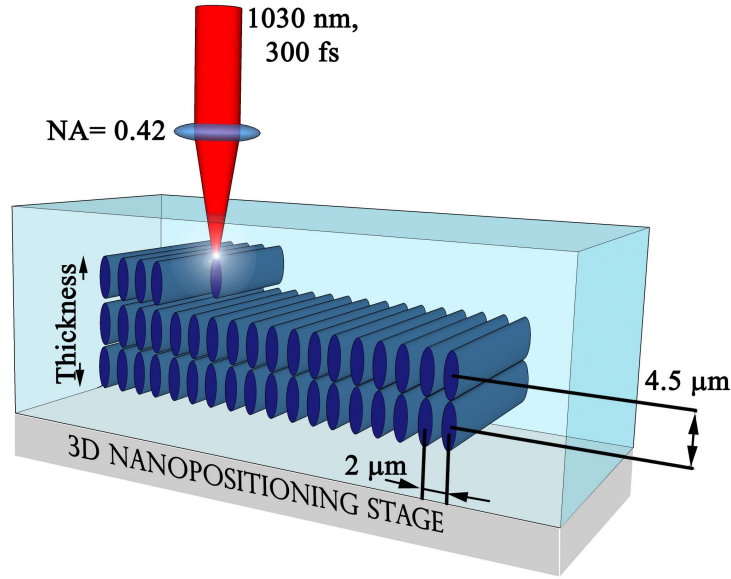
The VBG period ( $d$ ) and the wavelength ( $\lambda$ ) only determine the angle at which Bragg condition is satisfied, while refractive index modulation level ( $\Delta n$ ) and thickness ( $t$ ) decide the efficiency of the element. It is obvious that by choosing optimal design parameters it is theoretically possible to achieve diffraction efficiency equal to 100%. Using this equation it is possible to evaluate the refractive index modulation level when grating thickness is known. For the diffraction efficiency evaluation, we have measured intensity of the diffracted beam and compared it to the reference beam. For the reference, we slightly shifted crystal position moving the grating out of the beam and measured the intensity of the transmitted light. In this way losses due to reflections and crystal absorption were eliminated. For measurements we used HeNe (633 nm) laser beam falling at Bragg angle with polarization perpendicular to the grooves.

As efficiency is a pure sinusoidal function periodic in the product  $\Delta n t$  (Fig. 1.9, a), for a given  $\Delta n$  value, only gratings with specific thickness could operate with high diffraction efficiency (Fig. 1.9, b). That thickness could range from several microns for high refractive index modulation level ( $\Delta n > 0.1$ ) up to several hundred microns for low level ( $\Delta n < 0.001$ ). If the modulation level of the refractive index is unknown, the thickness of the VBG has to be found experimentally.

The VBG fabrication scheme is shown in Fig. 1.10. The period of the grating was chosen to be 2 μm as in such configuration each line would slightly overlap, achieving more close-to-sinusoidal refractive index modulation pattern. Sufficient thickness of the VBG is created by fabricating several layers of gratings on top of each other with some spacing (in our case the spacing was chosen to be 4.5 μm which guaranteed that each layer slightly overlaps). Gratings were recorded with average pulse energies from 150 nJ to 250 nJ and sample translating speed was set to 3 mm/s at 300 kHz pulse repetition rate. The first grating layer was formed 400 μm below the sample's surface.

As precise magnitude of refractive index modulation was unknown, several 1 mm



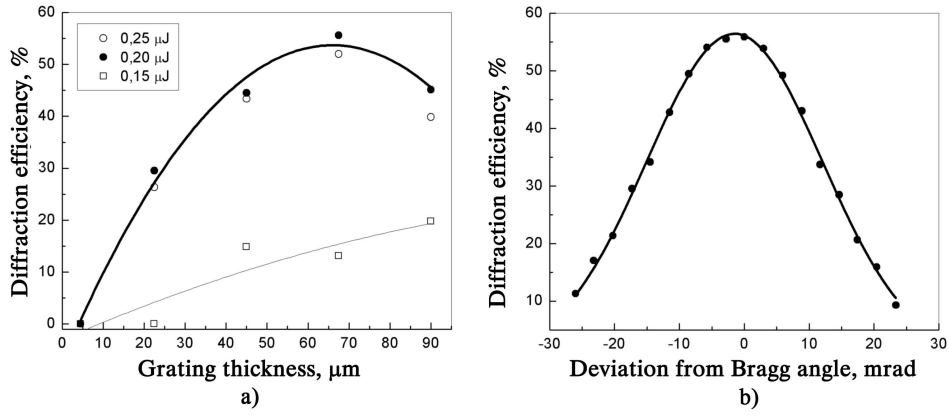


1.10 Fig: Schematic layout of fabricated volume Bragg grating.

$\times 1$  mm gratings with different thicknesses were fabricated. Their diffraction efficiencies are shown in Fig. 1.11, a). The efficiency was measured with 633-nm wavelength at angles satisfying Bragg condition thus giving the highest efficiency value. The measured Bragg angle was  $6.2^\circ$  and it perfectly coincides with theoretical value. The detuning from this condition results in rapid drop of the efficiency (Fig. 1.11, b). The maximum diffraction efficiency of 57 % was observed in a grating with 70- $\mu\text{m}$  thickness produced with 0.20- $\mu\text{J}$  laser writing energy.

By increasing (or decreasing) grating thickness the drop in efficiency is observed. It suggests that 70- micro m thickness is an optimal thickness which produces highest diffraction for given refractive index modulation level. By referring to Fig. 1.9, b), it is possible to evaluate the refractive index modulation level, which is  $0.0045 \pm 0.0007$ . By increasing writing power up to 0.25  $\mu\text{J}$  the overall efficiency slightly drops; however, maximum efficiency is observed at the same thickness. This suggests that by rising intensity no higher levels of uniform refractive index modification can be achieved as material damage starts to appear, increasing scattering level. When writing energy is lower, the modulation level is also smaller, so for 0.15  $\mu\text{J}$  the optimal thickness has to be higher and was not evaluated in this experiment. The manufacturing time of the VBG depends on the number of grating layers; a single 1 mm  $\times$  1 mm layer is fabricated in less than 3 minutes, though 70- $\mu\text{m}$ -thickness gratings are fabricated in less than 45 minutes.

There are two main reasons that prevent higher diffraction efficiencies of fabricated VBGs. First is a scattering of the incident beam from fabricated structure, caused by uniformity and scattering centers such as microdamages. The second cause is non-sinusoidally modulation of the refractive index change induced in the material. Theoretical models of VBG describe the sinusoidally modulated refractive index, however it is hard to achieve such distribution using direct laser writing technique as the modification profile after single shot is rather complicated, which means that



1.11 Fig: Diffraction efficiency dependence: a) on the grating thickness written with different pulse energies; b) on the detuning from the Bragg angle. All curves are fitted to the experiment data.

optimal writing conditions should be found experimentally. This suggests that even higher performance of the grating could be achieved by parameter optimization.



## 2 Modifications of refractive index in crystalline materials

Common types of glasses such as fused silica or borosilicate glass were mostly investigated for laser induced microstructuring. However, it was demonstrated that such structures can be created also in crystalline materials like lithium niobate [25]. Lithium niobate ( $\text{LiNbO}_3$ ) is one of the most important crystals used in nonlinear optics, and the ability to form embedded photonic elements in it could create new promising applications. Conventionally, the near-surface waveguides in  $\text{LiNbO}_3$  are created by ion diffusion techniques [26], but recently it was demonstrated that ultrafast laser pulses can also induce a sufficient refractive index change for waveguiding. It was reported that two types of refractive index modification can be induced in  $\text{LiNbO}_3$ , one of which is erasable after thermal annealing, while other remains permanent [27, 28]. Both these types can be utilized in practical applications, for example as erasable 3D data storage devices [29], or permanent waveguides [27]. The origin of these modifications is still under discussion: amorphization, crystalline structure destruction, and induced stresses around the modified zones are likable causes of the permanent variations of refractive index, whereas localized defect generation, and photorefractive effects at lower laser fluencies account for reversible modification [28, 30].

### 2.1 Photorefractive modifications in $\text{LiNbO}_3$ crystal

$\text{LiNbO}_3$  crystal has strong photorefractive effect first discovered in 1966 by Ashkin et al. [31]. When crystal is illuminated with strong radiation, electron excitation from valance (or defect) band to conductive band will start to appear. If illumination is inhomogeneous the charge gradient would build up and free-carrier migration would start forced by drift, diffusion and photovoltaic effects. These currents build an appreciable charge separation in the material that, naturally, creates electric space-charge field. This field induces refractive index changes due to the Pockels effect. For a space-charge field ( $E$ ) that is aligned along the optical axis of the material, refractive index change can be evaluated as

$$\Delta n_{o,e} = -\frac{1}{2}n_{o,e}^3 r_{13,33} E, \quad (2.1)$$

here  $n_{o,e}$  is ordinary or extraordinary refractive index, and  $r_{13,33}$  is electrooptical coefficients that for  $\text{LiNbO}_3$  crystal are 11 pm/V and 34 pm/V [32].

The charge separation in ferroelectric material is also inhomogeneous, because such crystals possess natural polarizability. Due to this effect in one crystal direction, charge migration will be highly efficient. This direction is usually called *c axis*, and in  $\text{LiNbO}_3$  this axis matches crystals optical axis. So the strongest charge separation and highest electric space-charge field appears along the *c axis*.

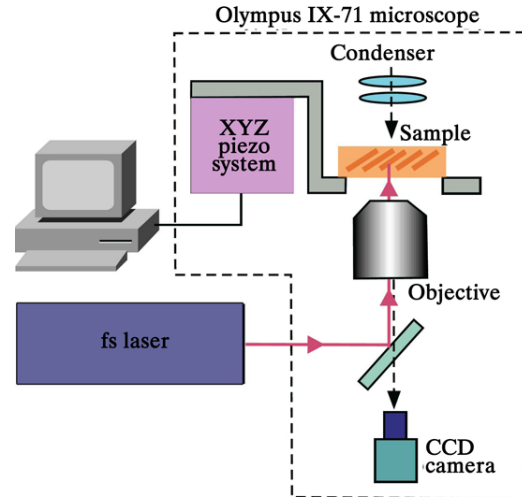
The magnitude of the electric-space charge field is proportional to the free carrier density. It was discovered earlier that doped crystals possess much stronger photorefractive effect. The extrinsic centers, created by dopants (usually transition metal dopants are used for this task with most popular one being iron (Fe)) enrich the total amount of free carriers and makes the photorefractive effect stronger. Pure  $\text{LiNbO}_3$  crystal is rarely used in photorefractive recordings.

Photorefractivity, induced with ultrashort laser pulses, was very scarcely investigated. It was only demonstrated, that it is possible to form three dimensional photorefractive structures in  $\text{LiNbO}_3:\text{Fe}$  crystals [29], also possibility to generate free carriers with IR wavelengths was also reported [33].

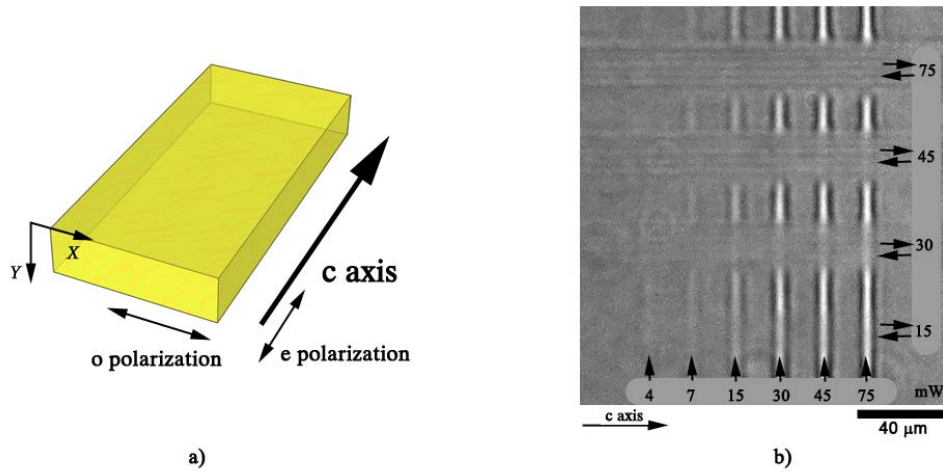
In our experiment, we used 800 nm wavelength and 150 fs duration radiation, generated from Ti:sapphire laser oscillator ("MaiTai", *Spectra Physics*). Impulse repetition rate was 80 MHz. The experiment scheme is depicted in Fig. 2.1. The sample was put on the three axis piezo nanopositioning stage (P-628, *PI*), having 800  $\mu\text{m}$  traveling range in XY direction, and 250  $\mu\text{m}$  in Z. The nanopositioning stage was combined with *Olympus IX-71* microscope, and laser beam was focused with the microscope objective. The real time monitoring of writing process was carried out with CCD camera. Before entering the microscope, laser beam was attenuated using atomized attenuator. Exposition was controlled with mechanical shutter.

Modifications were inscribed in Fe doped (0.05 %) and pure  $\text{LiNbO}_3$  crystals. Both crystals were Y-cut, and laser beam was perpendicular to crystal *c axis*. If the beam is translated perpendicular to the *c axis* the resulted refractive index modification will be clear, however, if the direction is parallel, modified zone becomes obscure. This effect is clearly illustrated in Fig. 2.2, b. When the sample translation direction is parallel to *c axis*, the previously recorded formations are modified. Employing this effect it is possible to use photorefractive material for three-dimensional data storage, where each information bit could be recorded and erased separately.

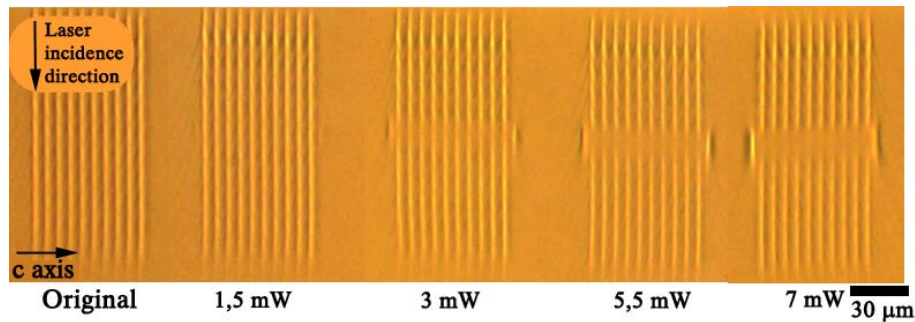
To test the possibility to selectively erase information from the volume of the material, thick grating was created in the bulk of the crystal (with the same technique used for VBG inscription in fused silica) and afterwards the middle layer was erased by changing sample translation direction. The results are shown in Fig. 2.3. These



2.1 Fig: Experimental scheme.



2.2 Fig: a) The main directions in LiNbO<sub>3</sub> crystal; b) microscope picture of modifications recorded in LiNbO<sub>3</sub>:Fe crystal with different translation directions and laser powers. Translation speed – 20 μm/s, objective – 0,3 NA, laser polarization – o.



2.3 Fig: Three dimensional data erasure in LiNbO<sub>3</sub>:Fe crystal. Thick gratings were recorded perpendicular to *c axis* (pulse average power – 7 mW, speed – 20 μm/s), and middle layer was erased by changing the writing direction to parallel to *c axis* (using 40 μm/s translation speed using different laser powers). Objective – 1,35 NA with immersion oil.

results demonstrate that it is really possible to erase the selected layer, while other layers remain intact. After erasure, information could be rewritten, however it was found out that the contrast of newly written information decreases, especially when the erasure procedure was repeated many times. The decrease of modification contrast after many erasure procedures are shown in Fig. 2.4. In order to understand the reasons, why such saturation effect is present in the crystal, it is important to analyze the topographical refractive index distribution in the crystal after the erasure procedure. In order to do that, the interferometer capable to measure refractive index changes and its distribution in the material was constructed, according to the schema shown in Fig. 2.5. The sample with recorded photorefractive modifications was illuminated with 635-nm wavelength cw laser, and the light, collected with objective (10x, 20x) was guided to the Michelson interferometer. A mirror in the one of the interferometer's arms was slightly misaligned in order to form clear interferometric

fringes in the output that was captured with CCD camera. By measuring the fringe deflection, it is possible to evaluate the refractive index change of the material: if the thickness of modified zone ( $\Delta z$ ) is known (measured with ordinary microscope), then  $\Delta n = \lambda\Phi/\Delta z$ , where  $\Phi$  is the deflection of fringes normalized to  $2\pi$ .

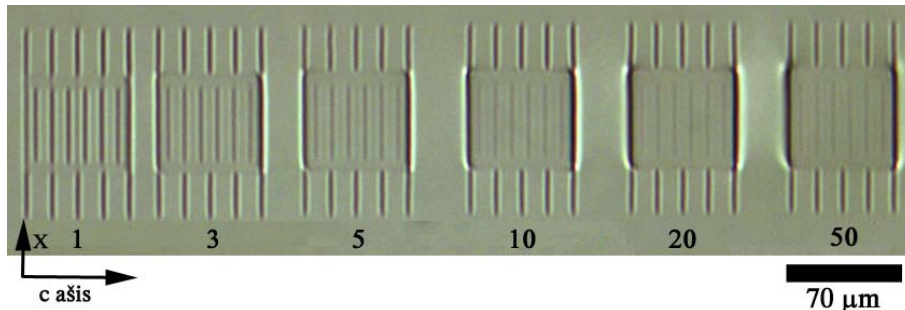
While inspecting the refractive index change distribution after erasure procedure, it was found out that erasure does not restore the original charge distribution, but only redistributes it to different geometry. After many erasure-writing repetitions, the maximum possible refractive index change build up in the material and no additional modification becomes possible. This phenomenon accounts for the previous mentioned saturation effect.

The induced refractive index change depends on the average pulse power, sample translation speed, focusing conditions and etc. When pulse repetition rate is high it is more convenient to use exposition dose expression:

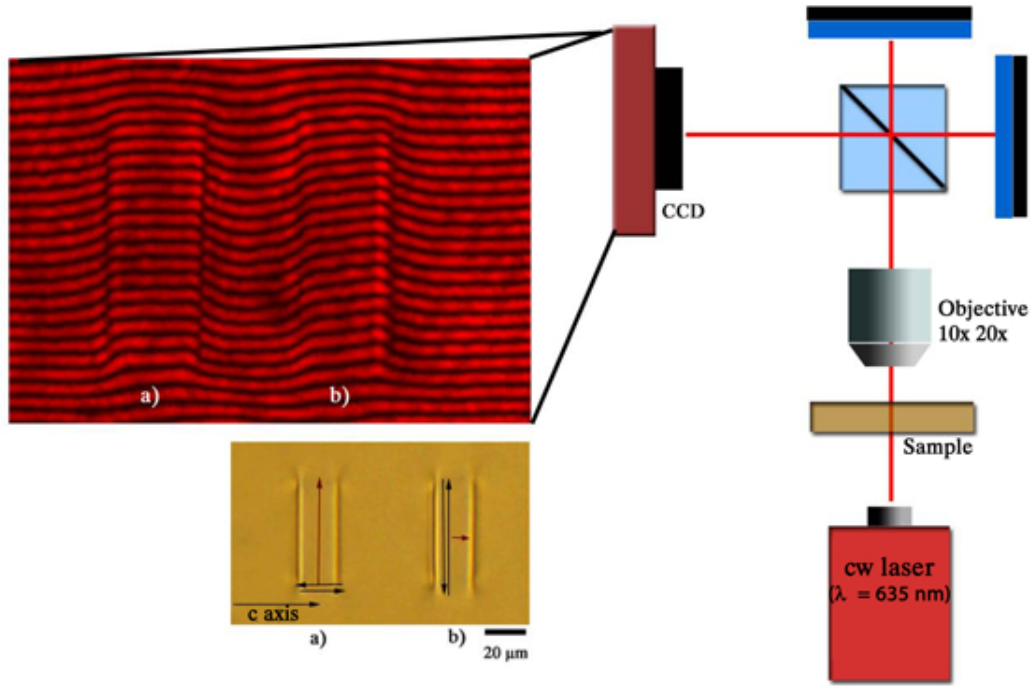
$$D = \frac{kP}{\pi r v}, \quad (2.2)$$

here  $P$  is average pulse power,  $v$  - translation speed,  $r$  - radius of modified structure. In order to increase exposition dose, it is possible to repeat the writing procedure several times in the same crystal area. The repetition number is denoted by  $k$  (if not mentioned otherwise,  $k = 1$ ).

The refractive index variations on the exposition dose are shown in Fig. 2.6. Also in Fig. 2.6, a) there is shown the results of evaluation of refractive index change using volume Bragg grating diffraction, as described in previous chapter. The highest diffraction efficiency was achieved in 350- $\mu\text{m}$  thickness grating and had 72 %. This corresponds to 0.0006 refractive index modulation level. This level is three times lower, if the incident beam polarization is not extraordinary – this proves that modification really have photorefractive origin, as electro-optic coefficient for  $o$  polarization is three times lower than  $e$  polarization. The refractive index change logarithmically grows with increasing exposition dose and starts to saturate when doses are high. The maximum refractive index change (in single modified line) was 0.0045 for  $\text{LiNbO}_3\text{Fe}$  crystal. It is interesting, that in pure  $\text{LiNbO}_3$  crystal it is also possible to create



2.4 Fig: Repetitive information recoding in  $\text{LiNbO}_3\text{:Fe}$ . The number shown in the picture shows how many times the rewriting procedure was repeated. Writing parameters: average power – 40 mW, translation speed – 20  $\mu\text{m/s}$ ; erasure parameters: average power – 75 mW, translation speed – 60  $\mu\text{m/s}$ . Objective – 0,3 NA.



2.5 Fig: The schema of Michelson interferometer used for refractive index change monitoring in the crystal. CCD camera takes images of interference fringes (inset shows the sample of two zones: a) when erasure was performed parallel to the *c axis*, b) when erasure was performed perpendicularly to *c axis*)

photorefractive index changes, however the maximum level is lower – 0.0015.

Such big refractive index changes are not common in photorefractive modifications, induced with cw or long pulses. The reason that could explain such increase is the efficient generation of polarons in the crystal after ultrafast pulse exposure. It is known that polarons can enhance the photovoltaic effect and contribute to stronger charge separation in the crystal [34]. Also high laser repetition rates can efficiently heat the crystal and induce piezoelectric effects involve in enhancing greater charge separation.

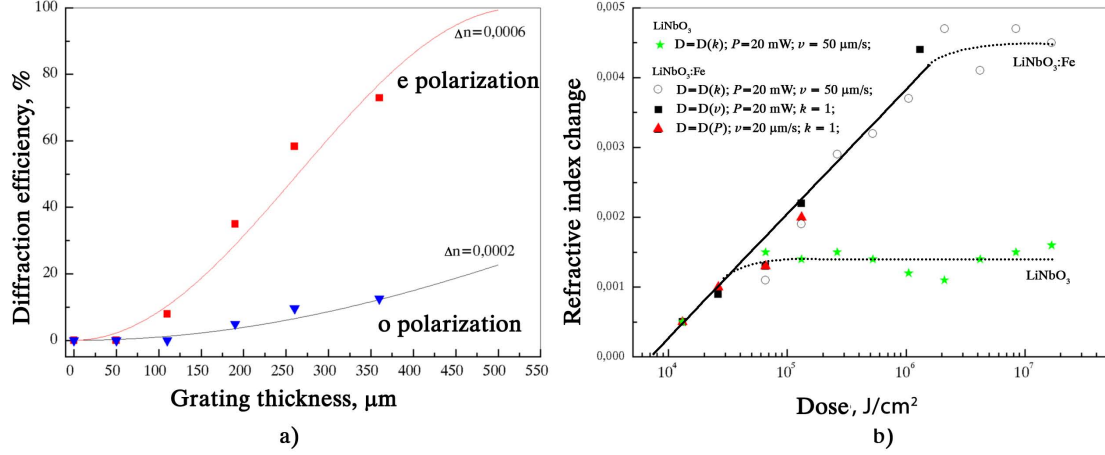
However, photorefractive modifications are not stable and can be completely erased using homogeneous UV light irradiation.

### 2.1.1 Permanent modifications induced in $\text{LiNbO}_3$

Photorefractive modifications become useless in applications orientated to high intensity pulses. Recorded structures, such as holograms, will be erased during read out procedure with intense radiation. Creation of permanent modifications in the crystals could solve these problems.

We have investigated the possibility to form stable modifications in  $\text{LiNbO}_3$  crystal, with Yb:KGW laser system. The experimental setup used for crystal modification was identical to the one used in glass modification experiments (refer to Fig. 1.1). We used pure congruent  $\text{LiNbO}_3$  crystal samples at z-cut orientation (mo-





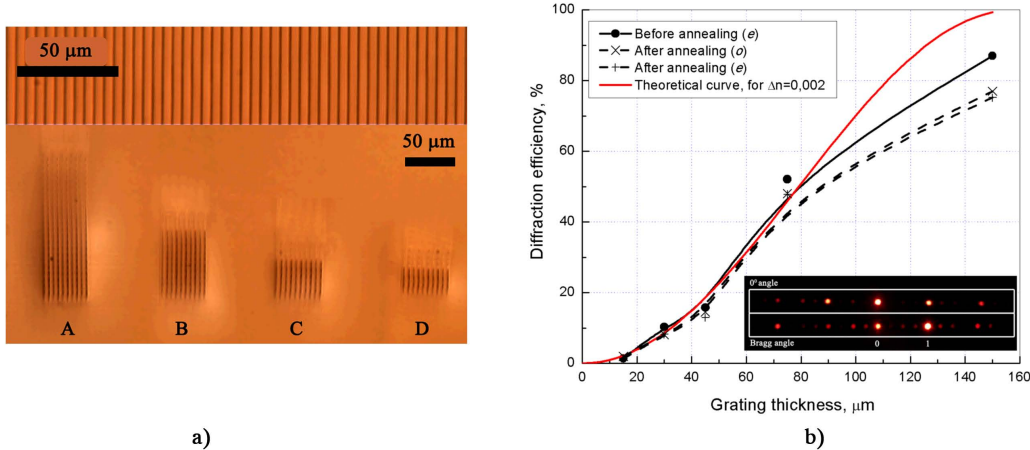
2.6 Fig: a) Diffraction efficiency of Bragg grating dependence on grating thicknesses and reading beam polarization. Gratings were recorded in  $\text{LiNbO}_3\text{Fe}$  crystal with  $2 \times 10^2 \text{ J}/\text{cm}^2$  exposition dose, period was  $6 \mu\text{m}$ . Continuous curves show theoretical values calculated using coupled wave theory. b) Refractive index change on exposition dose measured in pure  $\text{LiNbO}_3$  and  $\text{LiNbO}_3:\text{Fe}$ . Dose was varied by changing writing power ( $P$ ), translation speed ( $v$ ) or repeating writing algorithm ( $k$ ).

difications were written with the direction of propagation of the laser beam parallel to crystal's optical axis ( $\theta = 0^\circ$ ).

It is important to find the pulse energy window in which permanent index modifications can be created without increased scattering or absorption. For this task separate lines were formed in the bulk of the  $\text{LiNbO}_3$  crystal,  $200 \mu\text{m}$  below the surface. The visible modifications were observed with laser pulse energies as low as  $200 \text{ nJ}$ , but modifications, that did not disappear after thermal annealing (1 hour in  $150^\circ\text{C}$ ) were created with pulse energies higher than  $1.2 \mu\text{J}$  (corresponding to  $33 \text{ J}/\text{cm}^2$  energy density). It is important to note that in  $\text{LiNbO}_3$  the critical power for self-focusing is  $\approx 0.5 \text{ MW}$  for  $1030 \text{ nm}$ , ( $150 \text{ nJ}$  at  $300 \text{ fs}$ ) [35], meaning that modification recording in our experiment was affected by filamentation processes. Modifications were highly elliptical and axial length varied on focusing depth due to filamentation and spherical aberrations, and could reach sizes from  $8 \mu\text{m}$  close to surface up to  $20 \mu\text{m}$  at depths of  $500 \mu\text{m}$ ; focus splitting after repetitive self-focusing was also observed. The lateral width of induced modifications was  $\sim 1.5 \mu\text{m}$ .

The optimal sample translation speed was found to be  $5 \text{ mm}/\text{s}$  and this value was used in all experiments described below; slower speeds did not improve visible structure quality and at very low speeds ( $0.1 \text{ mm}/\text{s}$ ) the structure morphology even tended to decrease due to overexposure.

Three-dimensional gratings were inscribed in the crystal by translating the sample in respect to the incident laser beam. Several layers of gratings with slight separation were created on top of each other in order to create sufficient VBG thickness required for high diffraction efficiency (as shown in Fig. 1.10). In order to measure grating thicknesses, gratings were formed close to the crystal end-facets and inspected with transmission microscope.



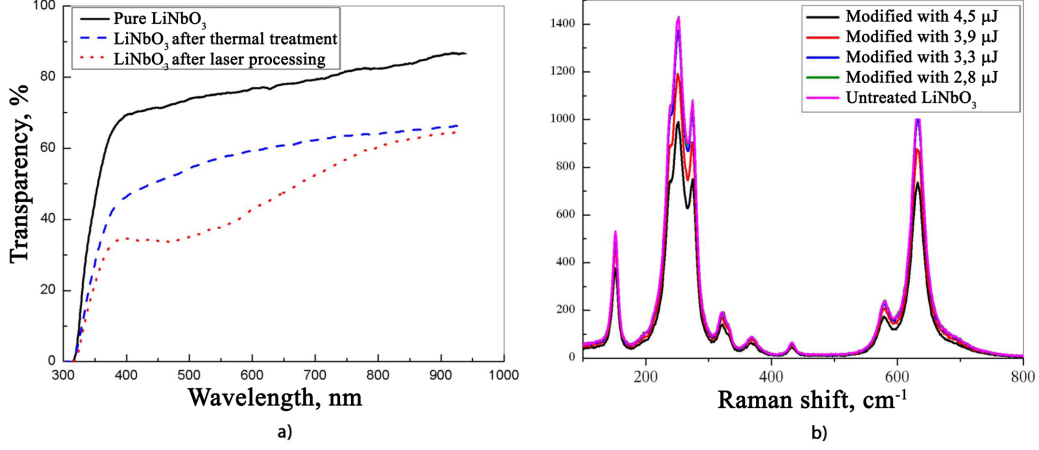
2.7 Fig: a) Fabricated VBG(*top*); side view of the sample gratings with different layer number: A) 20; B) 10; C) 5; D) 3; (*bottom*). Incident pulse energy – 3 μJ, translation speed – 5 mm/s, pulse repetition rate – 100 kHz. b) Diffraction efficiency dependence on the grating thickness. Gratings were written with 3 μJ pulse energy and 5 mm/s sample translation speed at 100 kHz pulse repetition rate. Inset shows the diffraction patterns for 0° and Bragg angle diffraction.

VBG's with 1-mm width and 1-mm length, 5-μm period and different thicknesses were manufactured in the LiNbO<sub>3</sub> crystal. The grating's first layer was created 320 μm below the surface, with all other layers were formed on top of each other with 7-μm separation. This separation was found to be optimal as it allowed complete overlapping of separate layers, thus axial elongation of the structures was beneficial in our case. Fabricated gratings are shown in Fig. 2.7, a). These gratings had thicknesses from 15 μm (one layer) up to 150 μm (20 layers).

The measured diffraction efficiency versus grating thickness is shown in Fig. 2.7, b). The grating with 150-μm thickness showed highest diffraction efficiency of 87 % for the first order, 2.5 % remained in the zero order, 7.5 % of diffracted intensities went to all higher orders, and 3 % was attributed to scattering losses. The evaluated refractive index modulation level was 0.002. By decreasing writing pulse energy down to 1.5 μJ, the maximum efficiency dropped to 56 %, suggesting the decrease of refractive index modulation level to 0.001. Similar refractive index modulations were reported by [28], induced with a 800-nm laser at fluencies comparable to these used in our experiment.

It was demonstrated by other groups [28], that refractive index modulation magnitude differs for ordinary (*o*) and extraordinary (*e*) beams in the crystal. This difference would make the diffraction efficiency of a grating polarization dependent. We could not observe this phenomenon in our experiment as diffraction efficiencies measured with parallel-to-the grooves polarized (*o*) light showed near identical (difference ~3 %) efficiencies as in the case of perpendicular (*e*) polarization.

The grating's impact on crystal's transmittance is shown in Fig. 2.8,a). Naturally, the grating induces scattering and diffraction losses in the crystal, reducing overall transmittance. A significant initial increase of the absorption can be seen in the visible region, peaking at 490 nm. However, this absorption band disappeared after



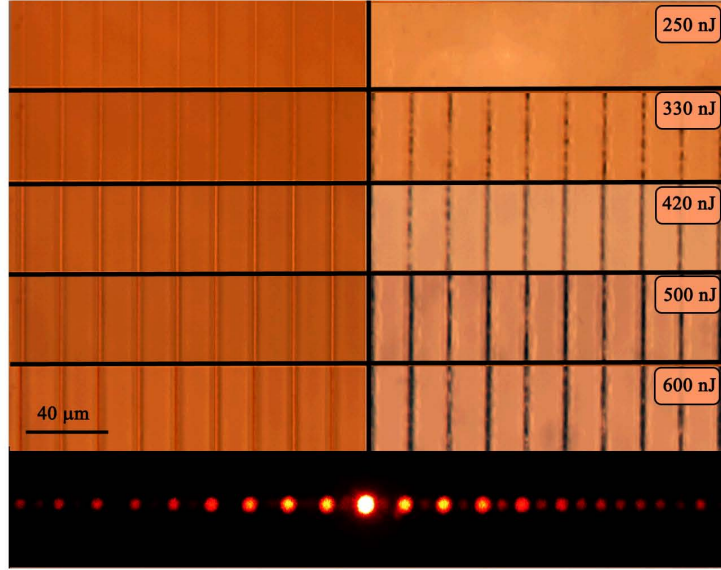
2.8 Fig: a) Transmittance versus wavelength for LiNbO<sub>3</sub> crystal, before and after inscription of the grating as well as after thermal annealing. Grating thickness was 15 μm (recorded with 3-μJ pulses, using 5 mm/s translation speed at 100 kHz pulse repetition rate). b) Raman spectra taken from laser-modified zones.

thermal annealing for 1 hour at 150°C. This peak is linked to the electron-trapped-in-oxygen-vacancy defect and is often observed in LiNbO<sub>3</sub> samples reduced at high temperature [36] or after exposure by high energy particles [37]. In the latter work the elimination of this coloration with thermal annealing, while keeping the refractive index modulation level relatively high was also reported. In our experiment the annealing also did not show great impact on the grating diffraction efficiencies; it decreased no more than 10 % for both polarizations, however, additional studies are required in order to test the stability behavior of the formed structures. Similar behavior occurs in the crystal after laser processing and ion exposure. This suggests a common cause of refractive index variations, which is mainly linked to the destruction of the lattice and partial amorphization at the laser processed zone. This theory is supported by the Raman spectra, taken from the laser-modified zones (Fig. 2.8, b). The intensity of Raman peaks decreases when crystal is affected by higher intensity pulses.

### 2.1.2 Modifications induced in KDP crystals

Identical experiments were performed with KDP crystal (crystal was cut at angle  $\theta = 58^\circ$ ). The laser pulse energy window for visual modification appearance was found to be from 250 nJ to 700 nJ (correspondingly from 7 J/cm<sup>2</sup> to 20 J/cm<sup>2</sup>). For lower intensities no visible structures were detected, whereas for higher intensity macrocracks, reaching 1 mm and more, start to appear in all processed regions. Crystal coloration was also observed at the crack zones. This coloration disappeared after several days. The critical self-focusing energy for KDP crystal was estimated to be 550 nJ. [35]. Filamentation effects were, therefore, minimal. The modification lateral width was  $\sim 3 \mu\text{m}$ , and the axial length was  $\sim 9 \mu\text{m}$ . Thermal annealing erased or considerably decreased structure morphology; the inhomogeneous lines acting





2.9 Fig: Modifications induced in a KDP crystal at various pulse energies. Modifications after thermal annealing are shown at the right for individual pulse energies (translation speed in all samples was 5 mm/s and pulse repetition rate - 100 kHz). The diffraction pattern from 20  $\mu\text{m}$  thick grating made with 600 nJ pulses is shown below.

as scattering centers are shown in Fig. 2.9. We were unable to create smooth regions of modified refractive index change, and Bragg diffraction was not observed in KDP crystal. Only amplitude gratings were formed with low diffraction efficiencies (26 % for all diffraction orders at  $0^\circ$  incident angle).

Despite a wide band gap and a high laser induced damage threshold (LIDT), microscopic fractures are formed in KDP as soon as laser intensity reaches the threshold for index of refraction modifications. In contrast  $\text{LiNbO}_3$ , which has a smaller band gap and lower LIDT, can withstand energy densities two orders of magnitude greater than the threshold of index modification. For comparison, the LIDT of KDP it is estimated to be  $5.5 \text{ J/cm}^2$  by the analysis of critical electron density [10] whereas that of  $\text{LiNbO}_3$  is  $0.7 \text{ J/cm}^2$ , and the band gap of KDP is 7 eV compared to 3.8 eV for  $\text{LiNbO}_3$ . It is known, however, that KDP crystal decomposes to water vapor and  $\text{KPO}_3$  salt at  $250^\circ\text{C}$  [38]. Such temperatures are easily reached at the laser focus. We speculate internal pressure caused by water vapor and repetitive laser heating could break the lattice structure and form both microscopic cracks and larger fractures.  $\text{LiNbO}_3$  does not have such a phase transition and the melted state is reached at  $1796^\circ\text{C}$ .

In conclusion, we have investigated the modifications induced in nonlinear crystals using high-repetition-rate, 300-fs-duration laser pulses. We have successfully fabricated high-efficiency volume Bragg gratings in  $\text{LiNbO}_3$  that remained permanent after at least one hour of thermal annealing in  $150^\circ\text{C}$ . It was not possible to create VBG's in KDP crystal due to inhomogeneous damage formation in the processed zone. The results with lithium niobate, in other hand, show potential for femtosecond-microprocessing of photonic devices, and considering the excellent nonlinear proper-

ties of LiNbO<sub>3</sub>, opportunities for new applications. Additional studies, however, are required with different laser processing parameters as well as research on annealing behavior of induced structures.

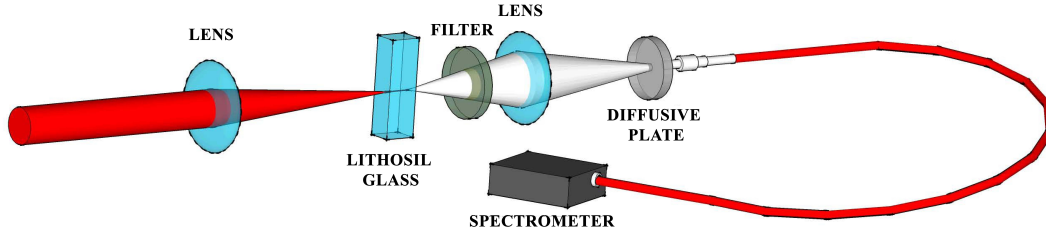
# 3 Fused silica modification with light filaments, and the influence of modified material on glass nonlinearities

Sharp focusing is capable to produce highly localized modifications in the bulk glass, having micrometer or sub-micrometer sizes. In other hand, small structures are not beneficial in this case when designed photonic element is big in size – the inscription procedure becomes too long. One favorable solution would be to use lens that has lower numerical aperture, capable to modify greater volumes of the material. However, weaker focusing requires higher laser power. High pulse power is cable to initialize the nonlinear processes in the material: filamentation, spectral broadening, supercontinuum generation and etc. The effects are determined not only by the laser power, but also by material properties, which as we know by now, are changing during modification process. Thus observation of nonlinear process and their dynamics during modification developing are essential for better understanding of physics, happening in the material.

## 3.1 Experimental

The setup used for modification induction and nonlinear process investigation is shown in Fig. 3.1. The previous mentioned *Pharos* laser system was used, so the laser wavelength was 1030 nm with pulse duration – 300 fs. The focusing distance of the lens used in the experiment was 200 mm. The laser beam diameter before the lens was 3.9 mm. The modification induction was performed in LITHOSIL glass that had 5 mm thickness. The confocal parameter of this lens was  $\sim 8$  mm so the focus could cover the full glass thickness, however, the sample was positioned at the place where the longest filament is formed (in that case geometrical focus was around 4 mm bellow the sample surface).

The spectral broadening effects were investigated with the fiber spectrometer (“AvaSpec2048”, *Avantes*). Before the input, infrared filter was used in order to attenuate the intensity of fundamental wavelength. Also the additional lens and diffusive plate was used in order to integrate the spatial spectra. During the spatial spectra measuring experiments filter, lens and diffusive plate were removed, and radiation from the filament was directly guided to spatial spectrometer (“Positive light”, *Spectra Physics*, gratings - 142 grooves/mm). Also filament formation in the glass was observed with microscope in real time.



3.1 Fig: Experiment setup for filament formation and supercontinuum generation in fused silica with *Pharos* laser system.

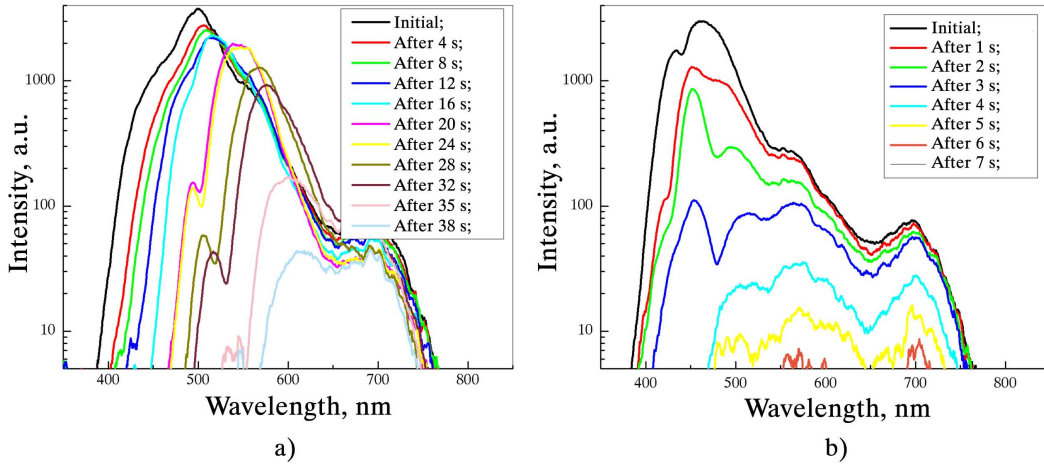
Filament formation experiment was carried out using different pulse repetition rates and pulse energies. The threshold energy for filament appearance (as well as supercontinuum) was  $3.5 \mu\text{J}$ , at 100 kHz. Similar energy was obtained with different pulse repetition rates. The critical peak power for filament formation is 4.1 MW in fused silica, and this correspond to 1.2 micro J energy (at 100 kHz). So in our experiment the observable supercontinuum started to appear when  $P = 2,9P_{kr}$ . When peak power reaches  $P = 7P_{kr}$ , homogeneous supercontinuum image decreases and interferometric patterns, caused by multiple filament formation, starts to appear. Most stable supercontinuum was achieved using peak powers 5–6 times greater than critical value.

## 3.2 Modification influence on supercontinuum spectra

When laser pulses expose the one singular area of the material, supercontinuum spectrum starts to change. These changes are linked with the appearance of modifications in the glass. The intensity of the supercontinuum starts to decrease, also the short-wavelength edge start to move to longer wavelengths. Typical spectral behavior is shown in Fig. 3.2. It is clear, that when pulse repetition rate is 100 kHz, modifications “shift” the supercontinuum edge from 400 nm to 550 nm in less than 40 s. This time is even shorter, with lower pulse energies. When exposition time is long enough, supercontinuum completely fades out and becomes undetectable. Results show, that modification indeed plays an important role in nonlinear processes happening in the material.

How induced modifications effect the supercontinuum? It is hardly possible to answer this question unambiguous, as the physics of supercontinuum formation is still unclear and negotiable. However, by analyzing supercontinuum generation theories it is possible to identify the processes that can be influenced by material modification.

Using the theory devised by Faccio er al. the blue-shifted supercontinuum, completely isolated from the pump wavelength is caused by the self-generated X-wave that forms during temporal pulse splitting [39]. Such X-wave travels in the material with group velocity that is considerably lower than velocity governed only by material dispersion. Such circumstance creates phase matching conditions and supercontinuum can be generated far from the pump wavelength. If we analyze supercontinuum’s



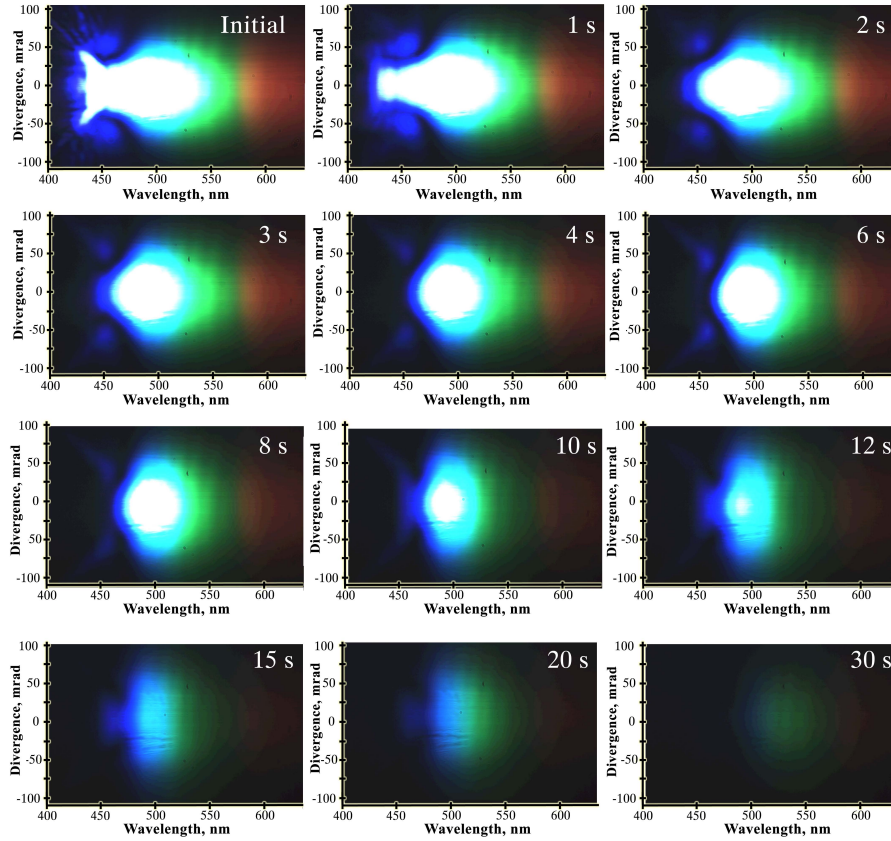
3.2 Fig: The dynamics of supercontinuum spectra during the exposition with 100 kHz laser pulses. Pulse peak powers are: a)  $5P_{kr}$  and b)  $4P_{kr}$ .

spatial spectrum, shown in Fig. 3.3, we will see that, indeed, X-shaped spectrum at the beginning of laser exposition is formed. However, such spectral formation disappears after sufficient exposition. It is known, that refractive index tend to increases in laser modified areas in fused silica, thus light filament is capable to create permanent waveguide. This waveguide can prevent the formation of X-wave packet, as it will trap the light and limit the conical radiation, essential for X-wave formation. So such behavior could explain the changes observed during in supercontinuum spectrum: decaying X-wave destroys the phase matching condition required for supercontinuum generation.

Also modification appearance in the glass could explain spectral shifts by using more traditional continuum generation models. It is commonly accepted, that the maximum supercontinuum broadening is determined by the intensity clamping. Maximum light intensity is limited in the core of the filament by nonlinear absorption. Also this clamping intensity is material property and can be expressed through nonlinear refractive index change. Blömer et. al. showed, that nonlinear refractive index in laser-modified fused silica decreases fivefold [40]. This automatically reduces clamping intensity and narrows the supercontinuum spectrum.

Also supercontinuum intensity tends to decrease after continuous exposition. The speed of attenuation is closely linked to the pulse repetition rate. When the rate is rather low ( $< 150$  kHz), attenuation speed is not well-defined and could vary from several seconds to minutes. Such behavior could be linked to the fluctuating laser power and not uniform distribution of defects in the material. However, when repetition rate is higher the attenuation speed is well defined. These results are shown in Fig. 3.4.

It is clear from the graph, that supercontinuum starts to generate instantly (at lower repetition, supercontinuum intensity growth was observed during the first 200 ms, however this growth was relatively small), and then follows continuous exponential attenuation with exposition time. At 160 kHz continuum generation stops after 3.5 s (measured at  $1/e^2$  level), while for 200 kHz it takes 850 ms, for 250 kHz – 250 ms



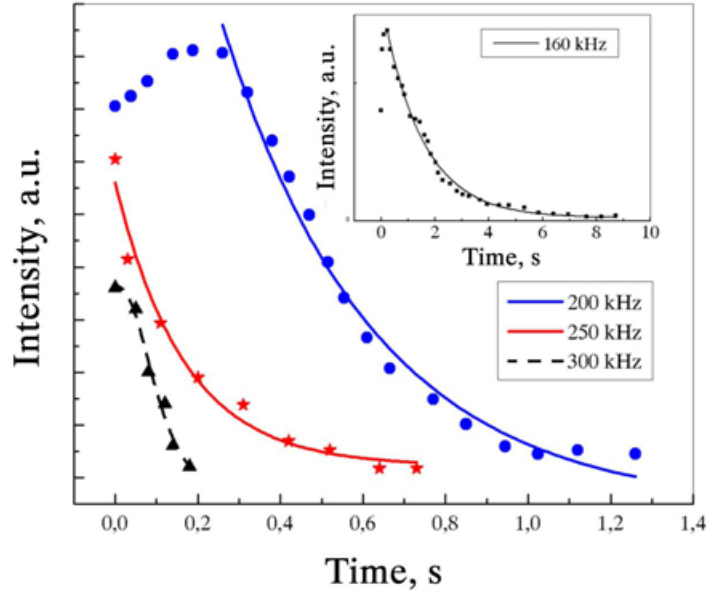
3.3 Fig: The change of spatial spectrum at various exposition times. Pulse peak power –  $7P_{kr}$ , pulse repetition rate – 100 kHz.

and for 300 kHz – 150 ms. These numbers show, that minimum number of pulses, required to affect the material and prevent the continuum generation decreases with increasing repetition rate. This shows the presence of accumulation effects, possible caused by shorty-lived defects in the material. It is known, that self-trapped excitons can efficiently form in the fused silica. The lifespan of such defect is shorter than 1 ms, and it is proven, that absorption properties of the material are influenced by these excitons [41,42]. These defects can increase modification formation rates when modifying with high repetition rate pulses.

### 3.2.1 Filaments and material modifications

Visual filament also splits into several parts along the pulse propagation direction, as can be seen from Fig. 3.5. The splitting has statistical behavior and is not always the same in identical conditions; however, main tendencies are always the same: visible observable purplish filament splits into two, three or more parts depending on the focusing conditions or used pulse powers.

Also this splitting appears only during single filament formation regime. When pulse power is higher than  $9P_{kr}$ , no such splitting is observed. It is important to stress that filament splitting forms during the first 2 s of exposition and later did not change. It is observed even when supercontinuum generation is already fading



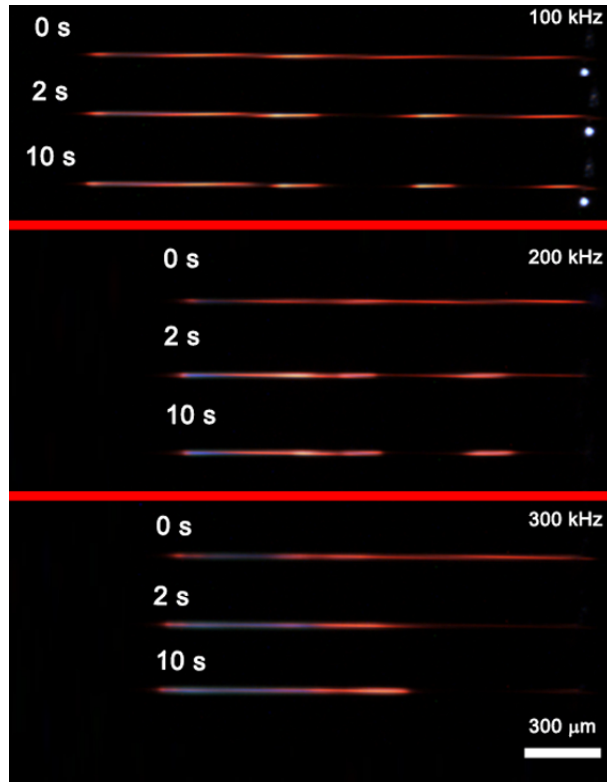
3.4 Fig: The supercontinuum intensity dependence on exposition time at various pulse repetition rates. Pulse peak power  $-5P_{kr}$ .

out. So the purplish glow of the filament is caused mainly by luminescence effect (non-bridged oxygen deficiency center fluoresces at 650 nm).

What causes filament splitting? It was discovered earlier, that intense filament core is surrounded with lower energy zone that acts like energy reservoir for sustaining the filament propagation [43]. Also Dubietis et al. showed, that if central filament part is blocked, filament tend to reconstruct itself after some propagation distance. However, if the reservoir is blocked, filament propagation is completely destroyed [44]. Modifications or material damage, that forms in the filament path could act as obstacles, disturbing filament propagation. Resulted modifications formed by filament, created with  $5P_{kr}$  peak power pulses and 100 kHz repetition rate are shown in Fig. 3.6 (microscope image taken in face contrast regime). The resulted modifications are not homogeneous along the filament propagation path and actually duplicate the original splitting of the filament. By close inspection it can be seen, that these modifications are located not precisely on the beam propagation path, but are slightly shifted in respect to each other. This suggests, that filament was deconstructed and later underwent reformation at some (or several) particular places. No obvious obstacle (as material damage) can be identified along the beam propagation path, however, in experiments with higher beam powers the material damage at places where filament breaks could be identified (such damages were observed and analyzed in detail by [45]). In other hand, just slight material modification, change of linear and nonlinear refractive index, could be sufficient for such filament breakage.

Also we can observe that modification length and their distribution are not identical even in the same recording conditions. This can cause problems when high modification placement accuracy is required. This could be a big drawback for some

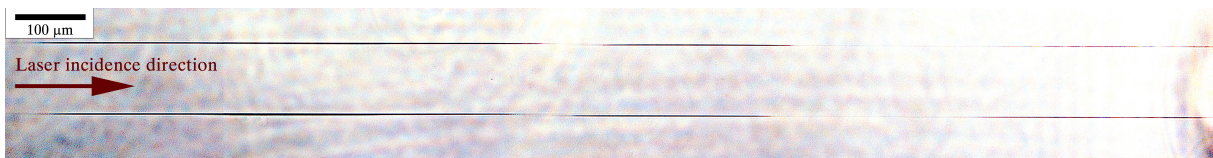




3.5 Fig: Splitting of the filament in the fused silica. Pulse peak power –  $5P_{kr}$ . Laser is incident from the left.

photonic devices fabrication. However, when accuracy is not the issue, modifications written with filaments could be beneficial, as it is possible to create various modification types with the filament [46], also some technical tasks can be simplified with filamentary recording, as in the case of precise positioning of modifications in the fiber core [47].

In conclusion we can state that with high pulse repetition rate Yb:KGW laser pulses it is possible to form modifications in fused silica using light filament. Modifications influence nonlinear processes, happening in the fused silica material. The supercontinuum spectrum rapidly changes when continuously exposing material, also filament splitting along the beam propagation is also present that fate the uneven distribution of formed modifications.



3.6 Fig: Modifications in fused silica written with laser filament. Average pulse power –  $5P_{kr}$ , repetition rate – 100 kHz.



# Conclusions

1. Modifications induced in fused silica glass with high repetition rate (100-300 kHz), 300 fs duration laser pulses, having wavelength of 1030 nm and energy densities over  $3 \text{ J/cm}^2$  possess birefringent effect caused by the nanograting (with period  $\approx 260 \text{ nm}$ ) formation in the laser-affected areas. Lower energy densities cannot create any permanent material modifications.
2. The regularity of modifications is fated by cumulating effects: nanograting homogeneity and repeatability depends on the number of pulses that targets the same material area which is determined by the pulse repetition rate and sample translation speed. In order to achieve homogeneous structure, each area should be targeted by at least 100 pulses (with energy densities in the range of  $3 \text{ J/cm}^2$  and  $5.6 \text{ J/cm}^2$ ). By increasing energy density the non-regular material damage is observed in material that increases overall scattering level. Effective refractive index change in the modified zones resulted from nanostructures was measured to be equal to  $0.0045 \pm 0.0007$  (for 633 nm wavelength).
3. In lithium niobate crystal it is possible to induce permanent, homogeneous modifications that have varied refractive index with ultrashort laser pulses. Modification window where smooth homogeneous modifications appear is between  $33 \text{ J/cm}^2$  and  $140 \text{ J/cm}^2$ . Modification threshold in lithium niobate crystal is one magnitude higher than that in fused silica due to the fact, that nonlinear refractive index is five times higher for niobate crystal that causes highly efficient filamentation process, disturbing the energy distribution at the focus. The cause of the refractive index change is local crystal amorphisation and values up to 0.002 can be reached.
4. In KDP crystal no homogeneous modifications can be created due to non-regular crystal decomposition into water vapor and  $\text{KPO}_3$  salt as soon as crystal damage threshold is reached at  $4 \text{ J/cm}^2$  energy density. Only amplitude gratings were recorded in this material.
5. Permanent volume Bragg gratings, that do not bear photorefractive character, and have record high diffraction efficiencies up to 78 % written in lithium niobate crystal using direct laser writing technique with Yb:KGW laser pulses (energy density  $85 \text{ J/cm}^2$ ) were demonstrated for the first time. In fused silica Bragg gratings had maximum diffraction efficiency of 57 % (written with  $5.6 \text{ J/cm}^2$ ).
6. The new method of laser-induced refractive index change evaluation is presented. This technique takes in advantage the fact that diffraction efficiency of Bragg grating is dependable on the grating thickness. When several gratings

with varied thicknesses are recorded with the same writing conditions, variation of diffraction efficiency on the thicknesses give clues about the magnitude of the refractive index change in the material. This method is simple and more precise than refractive index measurements from single fibers or thin diffraction gratings.

7. In the bulk of iron doped and pure lithium niobate crystals it is possible to induce photorefractive modifications with ultrashort, high repetition rate laser pulses, made with Ti:sapphire oscillator (wavelength - 800 nm, pulse duration - 150 fs, repetition rate - 80 MHz). Such unstable modifications can be created with energy densities as low as  $1 \text{ mJ/cm}^2$ . It was demonstrated for the first time, that in these crystals it is possible to selectively record and erase three-dimensional data using the same ultrashort laser system. The key process is nonlinear absorption that can be implemented for photorefractive data manipulation. The axial size of the written (and erased) bit depends on the total exposition dose and can vary from  $5 \text{ }\mu\text{m}$  (exposition dose -  $10^4 \text{ J/cm}^2$  and tight focusing (1.35 NA)) to  $70 \text{ }\mu\text{m}$  ( $10^5 \text{ J/cm}^2$  and loose focusing (0.3 NA)) The erasure of the recorded information is achieved by continuously increasing refractive index modulation level which with ultrashort pulses can reach up to 40 % higher values, than those obtained with longer pulse irradiation.
8. Light supercontinuum generated in fused silica with Yb:KGW laser pulses has blue-shifted spectrum (400-850 nm for 35 mm glass thickness, when using pulse powers where single filamentation regime is present) that is completely isolated from the pump pulse wavelength. Material modifications reduce the intensity of supercontinuum generation, and modifications cause the shift of shortwave supercontinuum edge towards longer wavelengths (from 400 nm up to 750 nm), that results in the shrinking spectrum of the supercontinuum. Experimentally evaluated spatial distribution of supercontinuum spectrum may suggest that changes in the spectrum can be caused by the decaying X-wave which becomes entrapped in the waveguide formed by the same light filament. The rate at which waveguide is formed depends on the laser repetition rate: supercontinuum generation stops after 150 ms since the beginning of exposition when pulse repetition rate is 300 kHz, and for 160 kHz this value is equal to 3,5 s.
9. Light filament-induced permanent modifications in fused silica are not homogeneously distributed along the filament path due to modulations that appear in the filament. Material modifications change pulse propagation conditions in the filament in such a way that filament is destroyed and should recreated itself after some distance. This causes uneven energy distribution along filament path that is also influenced by laser pulse parameters, such as laser pulse power and repetition rate.

# References

- [1] K. M. Davis, K. Miura, N. Sugimoto, and K. Hirao, Writing waveguides in glass with a femtosecond laser, *Opt. Lett.*, **21**(21), 1729–1731 (1996).
- [2] L. Sudrie, M. Franco, B. Prade, and A. Mysyrowicz, Study of damage in fused silica induced by ultra-short ir laser pulses, *Opt. Commun.*, **191**(3-6), 333–339 (2001).
- [3] E. N. Glezer, M. Milosavljevic, L. Huang, R. J. Finlay, T.-H. Her, J. P. Callan, and E. Mazur, Three-dimensional optical storage inside transparent materials, *Opt. Lett.*, **21**(24), 2023–2025 (1996).
- [4] R. Gattass and E. Mazur, Femtosecond laser micromachining in transparent materials, *Nat. Photonics*, **2**(4), 219–225 (2008).
- [5] K. Hirao and K. Miura, Writing waveguides and gratings in silica and related materials by a femtosecond laser, *J. Non-Cryst. Solids*, **239**(1–3), 91–95 (1998).
- [6] T. Toma, Y. Furuya, W. Watanabe, K. Itoh, J. Nishii, and K. Hayashi, Estimation of the refractive index change in glass induced by femtosecond laser pulses, *Opt. Rev.*, **7**(1), 14–17 (2000).
- [7] A. Schaap, Y. Bellouard, and T. Rohrlack, Optofluidic lab-on-a-chip for rapid algae population screening, *Biomed. Opt. Express*, **2**(3), 658–664 (2011).
- [8] LITHOSIL glass properties, <http://www.schott.com> (checked on 2011 09 21).
- [9] KV glass properties, <http://www.sciner.com/Opticsland/FS.htm> (checked on 2011 09 21).
- [10] H. Misawa and S. Juodkazis, *3D Laser Microfabrication: Principles and Applications* (WILEY-VCH, Weinheim, 2006).
- [11] E. G. Gamaly, S. Juodkazis, V. Mizeikis, H. Misawa, A. V. Rode, and W. Krolikowski, Modification of refractive index by a single femtosecond pulse confined inside a bulk of a photorefractive crystal, *Phys. Rev. B*, **81**(5), 054113(1–10) (2010).
- [12] L. Keldysh, Ionization in the field of a strong electromagnetic wave, *Sov. Phys. JEPT*, **20**(5), 1307–1314 (1965).
- [13] L. Sudrie, A. Couairon, M. Franco, B. Lamouroux, B. Prade, S. Tzortzakis, and A. Mysyrowicz, Femtosecond laser-induced damage and filamentary propagation in fused silica, *Phys. Rev. Lett.*, **89**(18), 186601(1–4) (2002).
- [14] N. Bloembergen, Laser-induced electric breakdown in solids, *IEEE J. Quantum Electron.*, **10**(3), 375–386 (1974).
- [15] V. R. Bhardwaj, E. Simova, P. P. Rajeev, C. Hnatovsky, R. S. Taylor, D. M. Rayner, and P. B. Corkum, Optically produced arrays of planar nanostructures inside fused silica, *Phys. Rev. Lett.*, **96**(5), 057404(1–4) (2006).
- [16] S. Richter, M. Heinrich, S. Döring, A. Tünnermann, and S. Nolte, Formation of femtosecond laser-induced nanogratings at high repetition rates, *Appl. Phys. A*,

- 104**, 503–507 (2011).
- [17] Y. Shimotsuma, P. G. Kazansky, J. Qiu, and K. Hirao, Self-organized nano-gratings in glass irradiated by ultrashort light pulses, *Phys. Rev. Lett.*, **91**(24), 247405(1–4) (2003).
- [18] D. Homoelle, S. Wielandy, A. L. Gaeta, N. F. Borrelli, and C. Smith, Infrared photosensitivity in silica glasses exposed to femtosecond laser pulses, *Opt. Lett.*, **24**(18), 1311–1313 (1999).
- [19] Q.-Z. Zhao, J.-R. Qiu, X.-W. Jiang, C.-J. Zhao, and C.-S. Zhu, Fabrication of internal diffraction gratings in calcium fluoride crystals by a focused femtosecond laser, *Opt. Express*, **12**(5), 742–746 (2004).
- [20] J. Arns, W. Colburn, and S. Barden, Volume phase gratings for spectroscopy, ultrafast laser compressors, and wavelength division multiplexing, *Proc. of SPIE*, **3779**, 313–323 (1999).
- [21] O. M. Efimov, L. B. Glebov, and V. I. Smirnov, High-frequency Bragg gratings in a photothermorefractive glass, *Opt. Lett.*, **25**(23), 1693–1695 (2000).
- [22] T. Tamaki, W. Watanabe, H. Nagai, M. Yoshida, J. Nishii, and K. Itoh, Structural modification in fused silica by a femtosecond fiber laser at 1558 nm, *Opt. Express*, **14**(15), 6971–6980 (2006).
- [23] K. Yamada, W. Watanabe, K. Kintaka, J. Nishii, and K. Itoh, Volume grating induced by a self-trapped long filament of femtosecond laser pulses in silica glass, *Jpn. J. Appl. Phys.*, **42**(11), 6916–6919 (2003).
- [24] H. Kogelnik, Coupled wave theory for thick hologram grating, *Bell Syst. Tech. J.*, **48**, 2909–2947 (1969).
- [25] L. Gui, B. Xu, and T. Chong, Microstructure in lithium niobate by use of focused femtosecond laser pulses, *IEEE Photonics Technol. Lett.*, **1**(5), 1337–1339 (2004).
- [26] G. L. Destefanis, J. P. Gailliard, E. L. Ligeon, S. Valette, B. W. Farmery, P. D. Townsend, and A. Perez, The formation of waveguides and modulators in  $\text{LiNbO}_3$  by ion implantation, *J. Appl. Phys.*, **50**, 7898–7905 (1979).
- [27] R. Thomson, S. Campbell, I. Blewett, A. Kar, and D. Reid, Optical waveguide fabrication in z-cut lithium niobate ( $\text{LiNbO}_3$ ) using femtosecond pulses in the low repetition rate regime, *Appl. Phys. Lett.*, **88**, 111109(1–3) (2006).
- [28] J. Burghoff, H. Hartung, S. Nolte, and A. Tuennermann, Structural properties of femtosecond laser-induced modifications in  $\text{LiNbO}_3$ , *Appl. Phys. A*, **86**(2), 165–170 (2007).
- [29] S. Juodkazis, M. Sudzius, V. Mizeikis, H. Misawa, E. G. Gamaly, Y. Liu, O. A. Louchev, and K. Kitamura, Three-dimensional recording by tightly focused femtosecond pulses in  $\text{LiNbO}_3$ , *Appl. Phys. Lett.*, **89**(6), 062903 (2006).
- [30] D. Deshpande, A. Malshe, E. Stach, V. Radmilovic, D. Alexander, D. Doerr, and D. Hirt, Investigation of femtosecond laser assisted nano and microscale modifications in lithium niobate, *J. Appl. Phys.*, **97**(7), 074316(1–9) (2005).
- [31] A. Ashkin, G. D. Boyd, J. M. Dziedzic, R. G. Smith, A. A. Ballman, J. J. Levinstein, and K. Nassau, Optically-induced refractive index inhomogeneities in  $\text{LiNbO}_3$  and  $\text{LiTaO}_3$ , *Appl. Phys. Lett.*, **9**(1), 72–74 (1966).
- [32] K. Onuki, N. Uchida, and T. Saku, Interferometric method for measuring electro-

- optic coefficients in crystals, *J. Opt. Soc. Am.*, **62**(9), 1030–1032 (1972).
- [33] O. Beyer, I. Breunig, F. Kalkum, and K. Buse, Photorefractive effect in iron-doped lithium niobate crystals induced by femtosecond pulses of 1.5  $\mu\text{m}$  wavelength, *Appl. Phys. Lett.*, **88**(5), 051120(1–5) (2006).
- [34] F. Jermann and J. Otten, Light-induced charge transport in  $\text{LiNbO}_3\text{:Fe}$  at high light intensities, *J. Opt. Soc. Am. B*, **10**(11), 2085–2092 (1993).
- [35] M. Weber, *Handbook of optical materials* (CRC Press, New York, 2003).
- [36] L. E. Halliburton, K. L. Sweeney, and C. Y. Chen, Electron spin resonance and optical studies of point defects in lithium niobate, *Nucl. Instrum. Meth. B*, **1**(2-3), 344 – 347 (1984).
- [37] B. Andreas, K. Peithmann, K. Buse, and K. Maier, Modification of the refractive index of lithium niobate crystals by transmission of high-energy  $^4\text{He}^{2+}$  and  $\text{D}^+$  particles, *Appl. Phys. Lett.*, **84**(19), 3813–3815 (2004).
- [38] K. Lee, Hidden nature of the high-temperature phase transitions in crystals of  $\text{KH}_2\text{PO}_4$ -type: Is it a physical change?, *J. Phys. Chem. Solids*, **57**(3), 333–342 (1996).
- [39] D. Faccio, A. Averchi, A. Lotti, M. Kolesik, J. V. Moloney, A. Couairon, and P. Di Trapani, Generation and control of extreme blueshifted continuum peaks in optical Kerr media, *Phys. Rev. A*, **78**(3), 033825(1–6) (2008).
- [40] D. Blömer, A. Szameit, F. Dreisow, T. Schreiber, S. Nolte, and A. Tünnermann, Nonlinear refractive index of fs-laser-written waveguides in fused silica, *Opt. Express*, **14**(6), 2151–2157 (2006).
- [41] P. Martin, S. Guizard, P. Daguzan, G. Petite, P. D’Oliveira, P. Meynadier, and M. Perdrix, Subpicosecond study of carrier trapping dynamics in wide-band-gap crystals, *Phys. Rev. B*, **55**(9), 5799–5810 (1997).
- [42] C. Itoh, K. Tanimura, and N. Itoh, Optical studies of self-trapped excitons in  $\text{SiO}_2$ , *J. Phys. C: Solid State Phys.*, **21**(26), 4693–4702 (1988).
- [43] S. Chin, A. Brodeur, S. Petit, O. Kosareva, and V. Kandidov, Filamentation and supercontinuum generation during the propagation of powerful ultrashort laser pulses in optical media (white light laser), *J. Nonlinear Opt. Phys. Mat.*, **8**(1), 121–146 (1999).
- [44] A. Dubietis, E. Kucinskas, G. Tamosauskas, E. Gaizauskas, M. A. Porras, and P. D. Trapani, Self-reconstruction of light filaments, *Opt. Lett.*, **29**(24), 2893–2895 (2004).
- [45] V. Kudriašov, *Nonlinear propagation of femtosecond pulses and induced modifications in optical glasses, PhD Thesis* (Vilniaus Universitetas, Lietuva, 2007).
- [46] I. Zergioti, K. D. Kyrkis, D. G. Papazoglou, and S. Tzortzakis, Structural modifications in fused silica induced by ultraviolet fs laser filaments, *Appl. Surf. Sci.*, **253**(19), 7865–7868 (2007).
- [47] M. Bernier, S. Gagnon, and R. Vallée, Role of the 1D optical filamentation process in the writing of first order fiber bragg gratings with femtosecond pulses at 800nm, *Opt. Mater. Express*, **1**(5), 832–844 (2011).

## SANTRAUKA

### LŪŽIO RODIKLIO MODIFIKAVIMAS STIKLUOSE IR KRISTALUOSE VEIKIANT ULTRATRUMPAISIAIS LAZERIO IMPULSAIS

Intensyvių šviesos impulsų sąveika su skaidriomis terpėmis iš esmės skiriasi nuo silpnos elektromagnetinės spinduliuotės sąveikos. Ultratrumpieji impulsai skaidrioje medžiagoje gali būti sugeriami, o sugertos energijos pakanka, kad medžiagoje įvyktų struktūriniai pokyčiai. Tokiu būdu pakinta ir medžiagos optinės bei fizikinės savybės. Selektyvus lūžio rodiklio modifikavimas leidžia integruoti įvairius fotoninius elementus į skaidriosios terpės tūrį. Tokia technologija yra itin svarbi fotonikos mokslo vystymuisi. Šioje disertacijoje ir nagrinėjama galimybė formuoti pakitusio lūžio rodiklio darinius lydyto kvarco stikle ir netiesiniuose kristaluose, tokiuose kaip ličio niobatas ar KDP.

Darbe pristatomi eksperimentiniai bei teoriniai rezultatai, susiję su skaidriųjų terpių lūžio rodiklio pokyčio indukavimu. Parodoma, kad lydytą kvarcą veikiant Yb:KGV lazerine sistema generuojamais impulsais, jame galima sukurti modifikuoto lūžio rodiklio sritis. Šios sritys pasižymi dvejopu šviesos lūžimu, atsirandančiu dėl medžiagos tūryje besiformuojančių nanogardelių. Parodoma, kad modifikuotų sričių vienalytiškumas priklauso nuo akumuliacinių efektų. Pakitusio lūžio rodiklio sritis taip pat galima įrašyti ir ličio niobato kristale. Priklausomai nuo spinduliuotės parametrų, šiame kristale galima įrašyti stabilius, modifikuoto lūžio rodiklio darinius, o taip pat ir nestabilias modifikacijas, atsirandančias dėl fotorefrakcinio reiškinių. Pastarąjį efektą galima panaudoti daugkartiniam informacijos įrašymui. Pademonstruoti efektyvūs fotoniniai elementai, turinės Brego gardelės, įrašytos tiek lydyto kvarco, tiek ličio niobato tūryje. Pateikiama metodika, skirta lazerio indukuoto lūžio rodiklio pokyčiui nustatyti matuojant Brego gardelių difrakcinius efektyvumus. Taip pat tyrinėjama kaip modifikuoti dariniai lemia superkontinuumo ir šviesos gijos formimosi reiškinius lydytame kvarce. Parodoma, kad besiformuojančios modifikacijos keičia superkontinuumo spektro parametrus: superkontinuumo spektras siaurėja, jo intensyvumas silpsta, be to, silpimas spartėja didėjant impulsų pasikartojimo dažniui. Taip pat vyksta trumpabangės superkontinuumo spektro ribos slinkimas link ilgesniųjų bangų. Stebimas šviesos gijos skilimas išilgai impulso sklidimo krypties.

## TRUMPOS ŽINIOS APIE DOKTORANTĄ

**Vardas:** Domas  
**Pavardė:** Paipulas  
*Gimimo data:* 1982 09 01  
*Gimimo vieta:* Panevėžys  
*Tautybė:* lietuvis  
*El. paštas:* domas.paipulas@ff.stud.vu.lt

### Išsilavinimas:

**1988-2000** Panevėžio Mykolo Karkos vidurinė mokykla.  
**2000-2004** Vilniaus universitetas, Fizikos fakultetas,  
*Bakaluro kvalifikacinis laipsnis (Cum laude diplomai).*  
**2004-2006** Vilniaus Universitetas, Fizikos fakultetas,  
*Magistro kvalifikacinis laipsnis.*  
**2007-2011** Vilniaus Universitetas, Fizikos fakultetas, Kvantinės  
elektronikos katedra. *Doktorantas.*

### Profesinė veikla:

**2005-2007** Lazerinių sistemų pardavimo vadybininkas,  
UAB EKSPLA.  
**2007-2011** Jaunesnysis mokslo darbuotojas, Lazerinių tyrimų centras.

## CURRICULUM VITAE

**Name:** Domas  
**Surname:** Paipulas  
*Date of birth:* 1982 09 01  
*Place of birth:* Panevėžys  
*Nationality:* lithuanian  
*E-mail:* domas.paipulas@ff.stud.vu.lt

### **Education:**

**1988-2000** Panevėžio Mykolo Karkos secondary school.  
**2000-2004** Vilnius University, Faculty of Physics. *Bachelor degree.*  
(*Cum laude*).  
**2004-2006** Vilnius University, Faculty of Physics. *Master degree.*  
**2007-2011** Vilnius University, Faculty of Physics, Department of  
Quantum Electronics. *PhD studies.*

### **Work experience:**

**2005-2007** Sales manager at EKSPLA Ltd. Responsible for  
laser and laser system sales for USA market.  
**2007-2011** Junior research fellow at Vilnius University  
Laser research center.